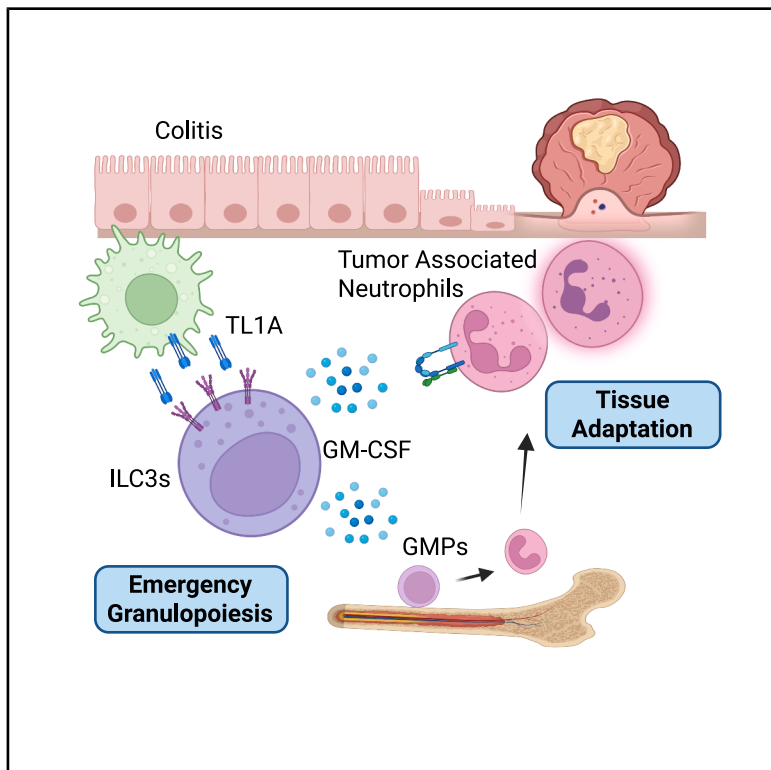


Immunity

Innate lymphoid cells activated by the cytokine TL1A link colitis to emergency granulopoiesis and the recruitment of tumor-promoting neutrophils

Graphical abstract



Authors

Sílvia Pires, Wei Yang, Sofia Frigerio, ..., Tracy L. Putoczki, Ian Wicks, Randy S. Longman

Correspondence

sdp4001@med.cornell.edu (S.P.), ral2006@med.cornell.edu (R.S.L.)

In brief

The incidence of colorectal cancer (CRC) is elevated in individuals with inflammatory bowel disease. Pires et al. find that the cytokine TL1A stimulates production of GM-CSF by ILC3s, which triggers emergency granulopoiesis and neutrophil recruitment and adaptation in inflamed tissue, thereby promoting inflammation-associated CRC.

Highlights

- TL1A stimulation of innate lymphoid cells promotes colitis-associated cancer
- TL1A-induced GM-CSF activates neutrophils with tumor-associated gene signatures
- Colitis and TL1A trigger emergency granulopoiesis via innate lymphoid cells
- Anti-TL1A therapy reduces neutrophil genes linked to tumor development

Article

Innate lymphoid cells activated by the cytokine TL1A link colitis to emergency granulopoiesis and the recruitment of tumor-promoting neutrophils

Sílvia Pires,^{1,*} Wei Yang,¹ Sofia Frigerio,^{2,3} Cynthia Louis,⁴ Chloe Scott,¹ Yu Lin Zhou,¹ Emre Cardakli,¹ Nancy Tran,⁵ Mina Hassan-Zahraee,⁶ Zhan Ye,⁶ Craig Hyde,⁶ Kenneth Hung,⁶ Amanda Chen,⁷ Charles Ng,⁸ Alexander Grier,¹ JRI Live Cell Bank,¹ Dana Lukin,⁵ Ellen Scherl,⁵ Stephan R. Targan,⁹ Gretchen E. Diehl,⁷ Joep Grootjans,^{2,3} Tracy L. Putoczki,⁴ Ian Wicks,⁴ and Randy S. Longman^{1,5,10,*}

¹Jill Roberts Institute for Research in Inflammatory Bowel Disease, Division of Gastroenterology and Hepatology, Department of Medicine, Weill Cornell Medicine, New York, NY, USA

²Department of Gastroenterology and Hepatology & Cancer Center Amsterdam, Amsterdam UMC, University of Amsterdam, 1105 AZ Amsterdam, the Netherlands

³Oncode Institute, Amsterdam, the Netherlands

⁴Walter and Eliza Hall Institute of Medical Research and Department of Medical Biology, University of Melbourne, Parkville, VIC, Australia

⁵Jill Roberts Center for Inflammatory Bowel Disease, Division of Gastroenterology and Hepatology, Weill Cornell Medicine, New York, NY, USA

⁶Pfizer Inc., Cambridge, MA, USA

⁷Immunology Program of the Sloan Kettering Institute, Memorial Sloan Kettering Cancer Center, New York, NY, USA

⁸Department of Pathology and Laboratory Medicine, Weill Cornell Medicine, New York, NY 10065, USA

⁹F. Widjaja Foundation Inflammatory Bowel Disease Institute, Department of Medicine, Cedars-Sinai Medical Center, Los Angeles, CA, USA

¹⁰Lead contact

*Correspondence: sdp4001@med.cornell.edu (S.P.), ral2006@med.cornell.edu (R.S.L.)

<https://doi.org/10.1016/j.jimmuni.2025.12.008>

SUMMARY

Inflammatory bowel disease (IBD) increases the risk of colorectal cancer (CRC). Genetic variants in *TNFSF15*, encoding tumor necrosis factor (TNF)-like cytokine 1A (TL1A), associate with severe IBD and advanced CRC. Here, we investigated how TL1A signaling promotes colitis-associated tumorigenesis. Deletion of the TL1A receptor in tissue-resident type 3 innate lymphoid cells (ILC3s) reduced colitis-associated tumorigenesis. TL1A signaling promoted neutrophil recruitment to the colon, which was required for tumor development. TL1A-stimulated ILC3s activated neutrophils, inducing a tumor-associated neutrophil (TAN)-like gene signature, and transfer of these neutrophils was sufficient to promote tumor growth. A similar TAN-like gene signature was enriched in human colitis-associated dysplasia but reduced following TL1A blockade in ulcerative colitis patients. Mechanistically, TL1A and colitis triggered emergency granulopoiesis, expanding granulocyte-monocyte progenitors and neutrophils in a manner dependent on ILC3-derived granulocyte-macrophage colony-stimulating factor (GM-CSF). Thus, a TL1A-ILC3-GM-CSF axis links colitis with emergency granulopoiesis and may serve as a therapeutic target to reduce colitis-associated CRC.

INTRODUCTION

Individuals with inflammatory bowel disease (IBD) are at increased risk for developing colorectal cancer (CRC), which contributes substantially to disease-associated morbidity and mortality. Unlike sporadic CRC, colitis-associated colorectal cancer (CAC) develops at a younger age and is associated with lower survival rates.^{1,2} The risk of CAC is closely linked to both the duration and the extent of colonic inflammation, highlighting the role of diffuse mucosal injury in promoting the development of cancers with molecular profiles distinct from those of sporadic CRC.^{3,4} Although several medical and biologic therapies are effective in managing ulcerative colitis (UC), the poten-

tial role of immune-mediated therapies in reducing CAC development remains poorly understood.

Tumor necrosis factor (TNF)-like cytokine 1A (TL1A), a member of the TNF superfamily, signals exclusively through its monogamous receptor death receptor 3 (DR3).⁵ Genetic variants in *TNFSF15*, which encodes TL1A, are associated with susceptibility to multiple autoimmune disorders and confer increased risk for more severe forms of IBD.⁶ TL1A is highly expressed in the colonic tissue during active colitis, and early evidence from recent clinical trials indicates that blockade of TL1A can attenuate inflammation in UC.⁷ TL1A is primarily expressed by myeloid cells in the intestine and its expression can be influenced by *TNFSF15* genetic variants.^{8–10} In addition to enhancing T cell

effector responses in synergy with co-stimulatory molecules, TL1A can modulate innate immune cell function through both autocrine and paracrine signaling in macrophages and innate lymphoid cells (ILCs).^{11–14} Although prior studies have linked elevated TL1A expression with tumor progression in gastric and CRC, the specific cellular and molecular mechanisms involved remain undefined.^{15,16}

Although neutrophilic infiltration of the colonic mucosa is a hallmark feature of active colitis, the mechanism that regulates the molecular and functional diversity of colonic neutrophils is only now emerging.¹⁷ Recent studies using spatial transcriptomic analyses revealed significant heterogeneity among neutrophils in IBD, suggesting that inflammation can shape tissue-specific adaptation of these cells.^{18,19} Tumor-associated neutrophils (TANs) also share this heterogeneity, exhibiting either pro- or anti-tumorigenic properties depending on the context.^{20,21} During both inflammation and cancer, increased neutrophil demand is met by stimulating a process called emergency granulopoiesis in the bone marrow.^{22,23} The signals linking colitis to this emergency granulopoiesis, as well as neutrophil tissue adaptation, remain poorly defined.

Here, we generated genetic mouse models to investigate the role of TL1A in CAC pathogenesis. Our findings demonstrate that TL1A signaling in ILC3s drives granulocyte-macrophage colony-stimulating factor (GM-CSF)-dependent neutrophil activation, a process that is essential for the development of colitis-associated tumors. Furthermore, we identify a previously unrecognized function for ILC3-derived GM-CSF in driving emergency granulopoiesis in the bone marrow and shaping colonic neutrophils capable of promoting tumor growth. These insights provide a mechanistic rationale for targeting TL1A in UC and may inform future precision medicine strategies aimed at preventing CAC in individuals with IBD.

RESULTS

Colitis-associated TL1A drives colorectal tumorigenesis

TL1A is highly expressed in human colonic tissue during active colitis,^{5,24} and emerging data from phase 2 studies have revealed the potential therapeutic efficacy of TL1A blockade in moderate to severe UC.^{25,26} Consistent with previous studies, tissue expression of TNFSF15 from the Cancer Genome Atlas (TCGA) database correlates with decreased long-term survival in subjects with CRC (Figure 1A).¹⁶ TL1A is highly expressed by CD11c⁺ mononuclear phagocytes (MNPs) in Crohn's disease²⁷ and mouse models of intestinal inflammation.¹¹ Similarly, in single-cell data from subjects with active UC, TNFSF15 is predominantly expressed by dendritic cells (DCs) and monocyte subsets (Figure 1B).^{9,11} TNFRSF25 (also called DR3), which is the receptor for TL1A, is primarily expressed by ILCs and T cells (Figure 1B).²⁸ To test the functional role of TL1A in a model of colitis-associated tumorigenesis, we utilized dextran sodium sulfate (DSS) treatment combined with a single injection of azoxymethane (AOM) to provide a reliable model of colitis-mediated CRC generation^{29,30} (referred to as AOM/DSS, Figure 1C). Although previous studies revealed that acute DSS exposure caused more severe colitis and weight loss in both DR3- and TL1A-deficient mice,¹¹ the reduced DSS exposure time of

5 days utilized here resulted in no significant differences in body weight over the experimental course (Figures S1A and S1B), enabling tumor assessment in this chronic model. Mice deficient in DR3 or with conditional deletion of TL1A in CD11c⁺ cells (called *Itgax*-cre *Tnfsf15*^{flox/flox}), which eliminates production of TL1A by intestinal MNPs,¹¹ also showed reduced tumor burden following AOM/DSS treatment compared with littermate controls (Figures 1D and 1E).

Although initial reports focused on T cells as the cellular target of TL1A, recent reports highlight a broader impact for TL1A on innate immune cells, epithelial cells, and fibroblasts.^{11,31–33} To evaluate the role of T cell-intrinsic TL1A signaling, *Cd4*-Cre *Tnfrsf25*^{flox/flox} mice, which lack DR3 expression on CD4⁺ T cells (Figure S1C), were subjected to AOM/DSS-induced tumorigenesis. These mice exhibited no differences in tumor number compared with littermate controls, indicating that TL1A may exert its pro-tumorigenic effects through non-T cell-dependent mechanisms (Figures 1F and S1D). To further explore the role of lymphocytes, *Rag1*^{−/−} mice deficient in DR3 were exposed to AOM/DSS alongside littermate controls. Despite comparable body weight loss across groups (Figure S1E), histological analysis revealed increased colitis severity in DR3-deficient mice (Figure S1F), consistent with previous work.¹¹ Despite this increased inflammation, these mice also showed a reduction in tumor burden as observed in the lymphoreplete model, reinforcing the conclusion that TL1A promotes tumorigenesis through signaling in innate immune cells rather than via adaptive immunity (Figure 1G).

TL1A enhances cytokine production by intestinal group 3 ILCs (ILC3s).^{34,35} To investigate the specific contribution of TL1A signaling in ILC3s to CAC, we used mice with targeted deletion of DR3 in ILC3s by crossing *Rorc*-Cre mice with *Tnfrsf25*^{flox/flox} mice, both on a *Rag2*-deficient background (referred to as DR3^{ΔILC3})¹¹ and a lymphocyte-sufficient background (referred to as DR3^{ΔRorc}), which targets DR3 both in ILC3s and Rorγt-expressing T cells (Figure S1G). Consistent with findings from DR3-deficient mice and DR3^{ΔILC3} mice,¹¹ DR3^{ΔRorc} mice also exhibited a modest increase in colitis severity even after a shorter 5-day exposure to DSS (Figure S1H). Despite the persistent evidence of intestinal inflammation, both DR3^{ΔILC3} and DR3^{ΔRorc} mice developed fewer tumors compared with littermate controls when challenged with AOM/DSS (Figures 1H and 1I). These findings support a pro-tumorigenic role for TL1A-driven ILC3 activity in the context of colitis.

TL1A-stimulated ILC3s promote TANs required for CAC

To evaluate the innate cells responsible for the pro-tumorigenic effect of TL1A, we performed flow cytometry of the colonic lamina propria cells. Flow cytometry showed reduced neutrophil infiltration in DR3-deficient mice compared with littermate controls (Figures 2A and S2A) but no difference in total CD45⁺ cells or CD11b⁺Ly6C^{hi} macrophages (Figure S2B). To further characterize the neutrophils in the colonic tissue microenvironment, we performed spatial transcriptomics using CosMx spatial molecular imaging on formalin-fixed paraffin-embedded (FFPE) tissue sections (Figures 2B and 2C). Eleven distinct cell clusters were identified, including neutrophils characterized by *S100a8/9* expression and several epithelial subsets expressing *Epcam* and *Krt19*, which included both colonocytes and neoplastic

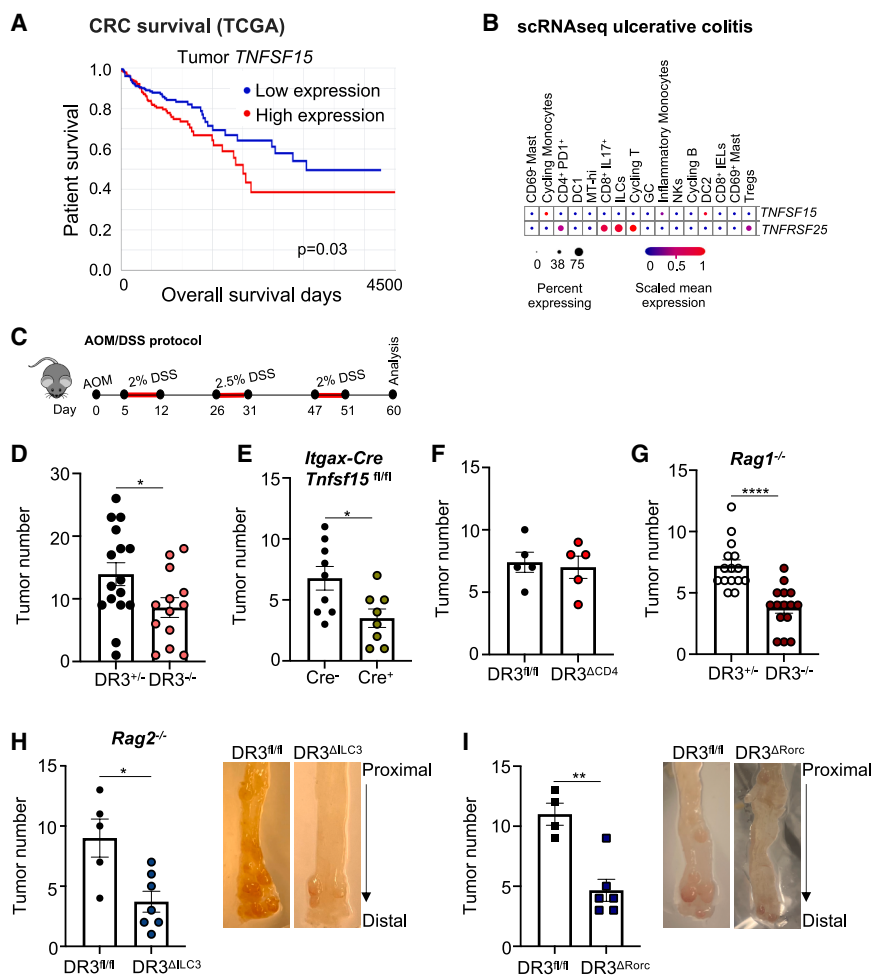


Figure 1. TL1A signaling in ILC3s promotes colitis-associated tumor development

(A) Kaplan-Meier survival curves for colon adenocarcinoma patients stratified by high vs. low *TNFSF15* expression in tumor tissue. TCGA data, $n = 448$.

(B) Expression of *TNFSF15* (TL1A) and *TNFRSF25* (DR3) within immune cells analyzed by single-cell RNA-seq of colon biopsies from healthy and ulcerative colitis (UC) subjects (from reference²⁸).

(C–I) Mice were injected with AOM followed by three cycles of DSS to induce colitis-associated tumorigenesis. (C) Schematic of the AOM/DSS protocol used in (D–I). (D) Tumor counts in colons of DR3^{+/−} heterozygous (Het) and DR3^{−/−} knockout (KO) littermate mice. Three pooled independent experiments (Het $n = 16$, KO $n = 13$). (E) Tumor counts in *Tnfsf15*^{fl/fl} (Het) and *Itgax-Cre Tnfsf15*^{fl/fl} (KO) mice. Two pooled independent experiments (Het $n = 9$, KO $n = 8$). (F) Tumor counts in *Tnfrsf25*^{fl/fl} (Het) and *Cd4-Cre Tnfrsf25*^{fl/fl} (KO) mice. Two pooled independent experiments (Het $n = 5$, KO $n = 5$). (G) Tumor counts in DR3^{+/−} (Het) and DR3^{−/−} (KO) littermate *Rag1*^{−/−} mice. Three pooled independent experiments (Het $n = 15$, KO $n = 16$). (H) Tumor counts in *Tnfrsf25*^{fl/fl} (Het) and *Rorc-Cre Tnfrsf25*^{fl/fl} (KO) *Rag2*^{−/−} mice. Two pooled independent experiments (Het $n = 5$, KO $n = 7$). Representative images of colonic tumors at the endpoint of AOM/DSS. (I) Tumor counts in *Tnfrsf25*^{fl/fl} (Het) and *Rorc-Cre Tnfrsf25*^{fl/fl} (KO) mice. Two pooled independent experiments (Het $n = 4$, KO $n = 6$). Representative images of colonic tumors at the endpoint of AOM/DSS.

Each dot represents an individual mouse (D–I). Data are presented as mean \pm standard error of the mean (SEM), and asterisks denote statistical significance ($*p < 0.05$, $**p < 0.01$, $****p < 0.0001$). Statistical significance was assessed using unpaired Student's t test (D, E, F, G, H, and I).

See also Figure S1.

epithelium marked by *Mmp7* and *Ifitm3* (Figure S2C). Neighborhood enrichment analysis revealed that DR3^{+/−} neutrophils preferentially co-localize with neoplastic epithelium rather than with colonocytes (Figure 2D).

Neutrophils are a pathologic hallmark of colitis and play a multifaceted role in CRC.³⁶ To determine whether neutrophils are required for TL1A-dependent colitis-associated tumorigenesis, we administered anti-Ly6G antibody to deplete neutrophils every 5 days over a 4-week period, beginning with the first cycle of DSS treatment. Effective neutrophil depletion was confirmed 24 h after the last round of anti-Ly6G depletion (Figure S2D). In wild-type (WT) mice, neutrophil depletion significantly reduced tumor burden following AOM/DSS treatment (Figure 2E). A similar reduction in tumor burden was observed in neutrophil-depleted *Rag1*-deficient mice, whereas no effect was seen in DR3-deficient mice, supporting a model in which neutrophils contribute to TL1A-mediated CAC.

To assess whether TL1A signaling is sufficient to induce colonic neutrophil recruitment, mice were treated with a previously validated agonistic anti-DR3 antibody.³⁷ Five days post-treatment, mice receiving the agonistic antibody showed enhanced neutrophil infiltration to the colonic lamina propria, even in the absence of intestinal inflammation, compared with

mice injected with an isotype control (Figure S2E). Because neutrophils do not express DR3 (Figure S2F), we predicted that TL1A was acting indirectly to mediate neutrophil recruitment to the colon. Consistent with a role for ILC3s, agonistic anti-DR3 failed to enhance neutrophil recruitment in DR3^{ΔILC3} mice (Figure 2F). To examine whether TL1A stimulated ILC3s directly influence neutrophil activation, we established an *in vitro* co-culture system using sorted intestinal ILC3s and bone-marrow-derived neutrophils (Figures 3A and S3A). Exposure to supernatants from TL1A-stimulated ILC3s, but not TL1A alone or unstimulated ILC3s, were sufficient to induce neutrophil activation, as indicated by upregulation of CD11b and CD177 (Figures 3A and 3B).

To determine the impact of TL1A-activated ILC3s on neutrophil function, we performed RNA sequencing (RNA-seq) of bone-marrow-derived neutrophils cultured with supernatants from intestinal ILC3s that were either unstimulated or stimulated with TL1A. Compared with neutrophils cultured alone or with supernatants from unstimulated ILC3s, exposure to TL1A-stimulated ILC3 supernatants induced distinct transcriptional changes in neutrophils evidence by principal coordinate analysis (Figure S3B). Differential expression analysis between TL1A-stimulated ILC3s and unstimulated supernatants revealed the upregulation of genes in neutrophils that were previously

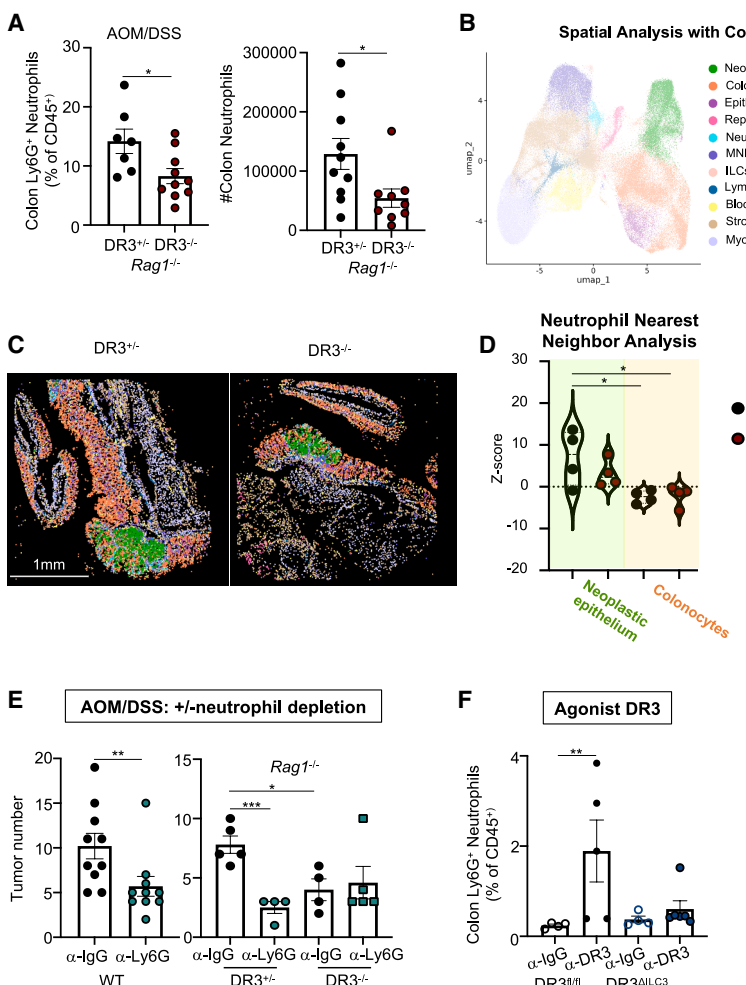


Figure 2. TL1A signaling recruits neutrophils essential for colitis-associated tumorigenesis

(A) Neutrophil infiltration in distal colon of DR3^{+/+} (Hets) and DR3^{-/-} (KO) *Rag1*^{-/-} mice. Two pooled independent experiments (Het $n = 7$ –10; KO $n = 9$ –10) following AOM/DSS.

(B–D) CosMx spatial molecular imaging of FFPE of colonic tissue from DR3^{+/+} and DR3^{-/-} *Rag1*^{-/-} mice following AOM/DSS (Het $n = 5$; KO $n = 5$). (B)

Uniform manifold approximation and projection (UMAP) visualization of CosMx for 103,337 cells from DR3^{+/+} and DR3^{-/-} *Rag1*^{-/-} mice. (C) Representative CosMx images showing probe signals for selected cell types corresponding to the UMAP clusters in (B). (D) Z score analysis of neighborhood enrichment between neutrophils and neoplastic epithelium or colonocytes.

(E) Tumor counts in WT and DR3^{+/+} or DR3^{-/-} *Rag1*^{-/-} mice treated with AOM/DSS and either anti-Ly6G (neutrophil-depleting antibody) or isotype control immunoglobulin (IgG). Two pooled independent experiments (WT: α-IgG [$n = 10$], α-Ly6G [$n = 10$]; Het: α-IgG [$n = 5$], α-Ly6G [$n = 4$]; KO: α-IgG [$n = 4$], α-Ly6G [$n = 4$]).

(F) Frequency of colonic neutrophils in *Tnfrsf25*^{fl/fl} (Hets) and *Rorc* Cre⁺ *Tnfrsf25*^{fl/fl} (KO) *Rag2*^{-/-} mice 5 days after treatment with agonistic α-DR3 or isotype control. One representative experiment out of two performed is shown (Het: α-IgG [$n = 4$], α-DR3 [$n = 5$]; KO: α-IgG [$n = 4$], α-DR3 [$n = 6$]). Each dot represents an individual mouse (A, D, E, and F). Data are presented as mean ± standard error of the mean (SEM), and asterisks denote statistical significance (* $p < 0.05$, ** $p < 0.01$). Statistical analysis was performed using unpaired Student's *t* tests (A and E) or one-way ANOVA with multiple comparisons (D and F).

See also Figure S2.

implicated in tumor initiation, growth, angiogenesis, and invasion (Figures 3C, S3C, and S3D).^{23,38,39} Notably, neutrophils exposed to TL1A-activated ILC3 supernatants expressed markers associated with TANs, such as *Cd14*, *Siglec*, and *Cebpb*—a transcription factor known to promote cancer progression.^{40–44} In addition, neutrophils exposed to TL1A-activated ILC3 supernatants exhibited increased expression of pro-inflammatory genes, including *I1b*, *Osm*, *Ptgs2* (COX-2), *Ccl2*, and *Mpo* (Figures 3C and S3C), all of which have been previously implicated in the initiation and progression of CAC.^{45–51} *In vivo* treatment with agonistic anti-DR3 antibody further confirmed the ability of TL1A signaling to induce colonic neutrophil expression of Siglec-F, PD-L1, and CD14, even in the absence of overt intestinal inflammation (Figure 3D).

Although reactive oxygen and nitrogen species produced by neutrophils are thought to contribute to precancerous mutations in UC and CRC,⁵² the early transcriptional signatures of colonic tumor-promoting neutrophils and their relationship to TL1A signaling remain poorly understood in humans. To investigate this, we performed digital spatial RNA profiling (DSP) of the CD45⁺ immune cells within a region of interest (ROI) of colonic dysplastic lesions from patients with or without IBD (Figure 3E; Table S3). DSP captures bulk gene expression

within the ROI, rather than single-cell resolution. A curated set of TAN signature genes (*CD14*, *CEBPB*, *MPO*, *OSM*, *CCL2*, *ICAM1*, and *IL1B*) identified from the transcriptional analysis above and published literature⁴⁴ were analyzed in IBD-associated dysplasia compared with sporadic dysplasia. In regions of dysplasia, CD45⁺ lamina propria immune cells from individuals with colitis-associated dysplasia showed a significant enrichment in the composite mean Z score of the neutrophil signature genes (*CD14*, *CEBPB*, *MPO*, *OSM*, *CCL2*, *ICAM1*, *IL1B*, and *VEGFA*), compared with those individuals with sporadic dysplasia (Figure 3F; Table S4). This included significant upregulation in *CEBPB*, *OSM*, and *CD14* (Figure S3E). To explore the potential role of TL1A in driving this TAN-like signature *in vivo*, we analyzed previously collected RNA-seq data from colonic biopsies of subjects with moderate to severe UC before and after 14 weeks of anti-TL1A therapy.²⁵ Consistent with a role for TL1A-dependent regulation of inflammatory neutrophil genes, treatment resulted in downregulation of key markers, including *OSM*, *MPO*, *IL1B*, *CCL2*, *PTGS2* (COX2), *CD14*, and *CEBPB*, as well as *CSF2* (Figure 3G). Collectively, these results provide evidence for the enrichment of TAN signature genes in colitis and colitis-associated dysplasia, which can be diminished by TL1A blockade.

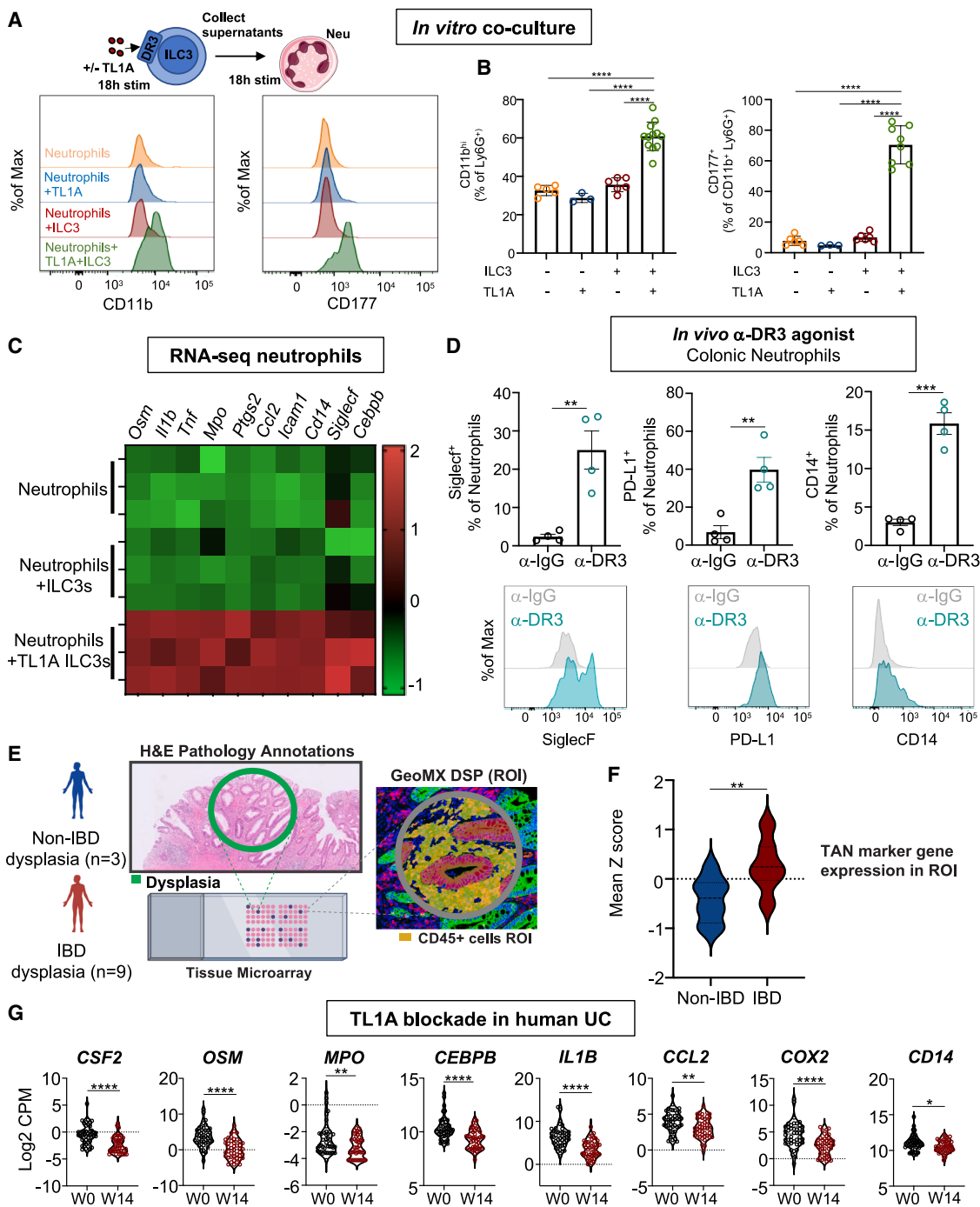


Figure 3. TL1A-stimulated ILC3s activate neutrophils and promote a TAN gene signature

(A–C) Bone-marrow-derived neutrophils were stimulated with supernatants of sorted colonic ILC3s, stimulated or not with TL1A. (A) Schematic of the experimental approach used in (B) and (C). Representative histograms show CD11b and CD177 expression levels on neutrophils following co-culture. (B) Surface expression of CD11b and CD177 on neutrophils cultured alone or after co-culture with ILC3 supernatants. One representative experiment out of ten performed is shown. (C) RNA-seq of bone-marrow-derived neutrophils stimulated for 18 h with supernatants from sorted intestinal ILC3s previously cultured \pm TL1A. Displayed are expression levels of genes associated with tumor-associated neutrophils (TANs).

(D) Frequencies of SiglecF, PD-L1, and CD14 expression in colonic neutrophils following injection of agonistic α -DR3 or isotype control antibody. One representative experiment out of three performed is shown ($n = 4$ per group).

(E and F) Digital spatial profiling performed on dysplastic colonic tissue from non-IBD and IBD patients. (E) Schematic of the experimental approach used in F. (F) Mean Z scores quantifying enrichment of the neutrophil gene signature in dysplastic lesions from non-IBD patients ($n = 3$, blue) versus IBD patients ($n = 9$, red).

(legend continued on next page)

To test the tumor-promoting capacity of neutrophils conditioned by TL1A-stimulated ILC3s *in vivo*, we adoptively transferred congenically marked ($CD45.1^+$) bone-marrow-derived neutrophils into $Rag1^{-/-}$ DR3 $^{-/-}$ mice undergoing AOM/DSS treatment (Figure 4A). Mice received intravenously either unstimulated neutrophils (Neu) or neutrophils pre-exposed to supernatants from TL1A-stimulated intestinal ILC3s (TL1A-Neu) every 7 days for 4 weeks, beginning with the first cycle of DSS treatment (Figure 4A). Homing of injected neutrophils to the colon was confirmed in DSS-treated mice and remained detectable 24 h post-injection (Figure S3F). Mice receiving TL1A-Neu exhibited a significant increase in tumor number in DR3 deficient mice, supporting the tumor-promoting role of neutrophils conditioned by TL1A-activated ILC3s (Figure 4B). To further investigate the pro-tumorigenic potential of neutrophils derived from an inflamed intestinal environment, we established a heterotopic tumor model using MC38, a murine CRC cell line. Neutrophils were isolated from the colons of WT mice following DSS-induced colitis and co-injected with MC38 cells subcutaneously (Figure 4C). Addition of 5×10^4 colonic neutrophils enhanced heterotopic tumor growth, compared with MC38 cells alone (Figure 4D), indicating that colitis-primed neutrophils can directly contribute to tumor progression.

To further test the tumor-promoting capacity of colonic neutrophils induced by TL1A signaling *in vivo*, colonic neutrophils were sorted from $Rag1^{-/-}$ DR3 $^{+/-}$ or $Rag1^{-/-}$ DR3 $^{-/-}$ exposed to DSS for 5 days and co-injected with MC38 to assess heterotopic growth (Figure 4E). Colonic neutrophils from $Rag1^{-/-}$ DR3 $^{+/-}$ mice increased heterotopic tumor growth compared with colonic neutrophils from $Rag1^{-/-}$ DR3 $^{-/-}$ mice (Figure 4F), demonstrating that TL1A signaling *in vivo* modulates the tumor-promoting capacity of these neutrophils.

TL1A promotes colitis- and ILC-dependent emergency granulopoiesis

During inflammation and cancer, the increased demand for neutrophils in peripheral tissues is met by enhanced production of neutrophils in the bone marrow through a process called emergency granulopoiesis.^{22,23} This process involves the expansion and differentiation of bone marrow progenitor cells, including LSK cells (Lin^- , Sca-1 $^+$, and c-Kit $^+$) and granulocyte-monocyte progenitors (GMPs; Lin^- , Sca-1 $^-$, c-Kit $^+$, CD150 $^-$, CD16/32 $^+$, and CD34 $^+$). Within the LSK compartment, the CD48 $^+$ CD150 $^-$ multipotent progenitor (MPP) population comprises, among others, myeloid-biased progenitors (MPP3) and lymphoid-biased progenitors (MPP4) (Figure S4A). During emergency granulopoiesis, MPP3s expand at the expense of MPP4s, promoting increased generation of GMPs to meet neutrophil demand. As previously shown,⁵³ both GMPs and neutrophils are expanded in the bone marrow of WT mice following 6 days of DSS-induced acute colitis, indicating colitis-induced granulopoiesis (Figure 5A). A similar expansion of GMPs and neutrophils was observed in $Rag2^{-/-}$ mice, which

lack lymphocytes, whereas this response is absent in $Rag2^{-/-}$ $Il2rg^{-/-}$ mice, which additionally lack ILCs, implicating ILCs in mediating the link between intestinal inflammation and emergency granulopoiesis (Figure 5B). In addition to colitis, administration of agonistic anti-DR3 antibody is sufficient to induce bone marrow granulopoiesis as compared with isotype control antibody (Figures 5C, 5D, and S5B). Further supporting a link between TL1A signaling and emergency granulopoiesis, bone marrow profiling 1 day after anti-DR3 treatment revealed an increase in myeloid-biased progenitors MPP3s, with a concomitant decrease in the lymphoid-biased MPP4s progenitors (Figure S5C). To investigate whether TL1A signaling modulates transcriptional regulators of granulopoiesis, we sorted LSK cells (Lin^- , Sca-1 $^+$, and c-Kit $^+$) and GMPs (Lin^- Sca-1 $^-$ c-Kit $^+$ CD150 $^-$ CD16/32 $^+$ CD34 $^+$) from WT mice 1 day after agonistic anti-DR3 treatment. TL1A stimulation significantly upregulated *Cebpb*, the key transcription factor controlling emergency granulopoiesis in GMPs (Figure 5E), while simultaneously downregulating *Cebpa*, the transcriptional driver of homeostatic granulopoiesis, in both LSKs and GMPs (Figure S4D).^{22,54} These findings support a role for TL1A in selectively promoting emergency granulopoiesis through transcriptional regulation of progenitors.

Hematopoietic progenitor cells, including LSKs and GMPs, do not express DR3 (Figure 5F), suggesting a role for another cell type in driving TL1A-dependent emergency granulopoiesis. Consistent with our observations in acute colitis, administration of agonistic anti-DR3 antibody induced the expansion of GMPs in $Rag2$ -deficient mice but not in $Rag2/Il2rg^{-/-}$ (Figure 5G). To specifically test the contribution of ILC3s, we examined the bone marrow in DR3 $^{\Delta ILC3}$ mice. In these mice, agonistic anti-DR3 treatment failed to induce expansion of GMPs and neutrophils in contrast to littermate controls (Figures 5H and S4E), highlighting a critical role for ILC3s in mediating TL1A-driven emergency granulopoiesis.

In patients with IBD, *TNFSF15* gene risk variants are associated with an increased likelihood of developing more severe disease phenotypes, including penetrating, fibrostenotic, and perianal disease complications.^{55,56} Individuals with these risk variants and CRC have also been shown to have higher TL1A expression in intestinal tissue, which correlates with more invasive cancer and metastases.¹⁶ Although individuals carrying risk alleles may exhibit lower baseline *TNFSF15* expression in myeloid cells,¹⁰ inflammatory stimuli can lead to heightened *TNFSF15* induction in these individuals.^{8,14} To test the potential relationship between the *TNFSF15* risk variants and granulopoiesis, we evaluated GMP frequencies in the Lin^- CD34 $^+$ peripheral blood progenitors of individuals with IBD (Figure S5), which previous studies have shown are representative of bone marrow progenitor populations.⁵⁷ Individuals harboring risk variants had a higher frequency of GMPs within the circulating progenitor cells and a higher number of neutrophils in the peripheral blood (Figures 5I and 5J). These results further support the potential

(G) Expression of CSF2 and TAN marker genes from colonic biopsies from UC subjects at baseline (week 0) and after 14 weeks of anti-TL1A therapy. Each dot represents data from an individual mouse (D) or patient sample (G). Values are presented as mean \pm standard error of the mean (SEM), and asterisks denote statistical significance (* $p < 0.05$, ** $p < 0.01$, *** $p < 0.001$, **** $p < 0.0001$). Statistical analysis was performed using unpaired Student's *t* tests (D, F, and G) or two-way ANOVA (B) with multiple comparisons.

See also Figure S3.

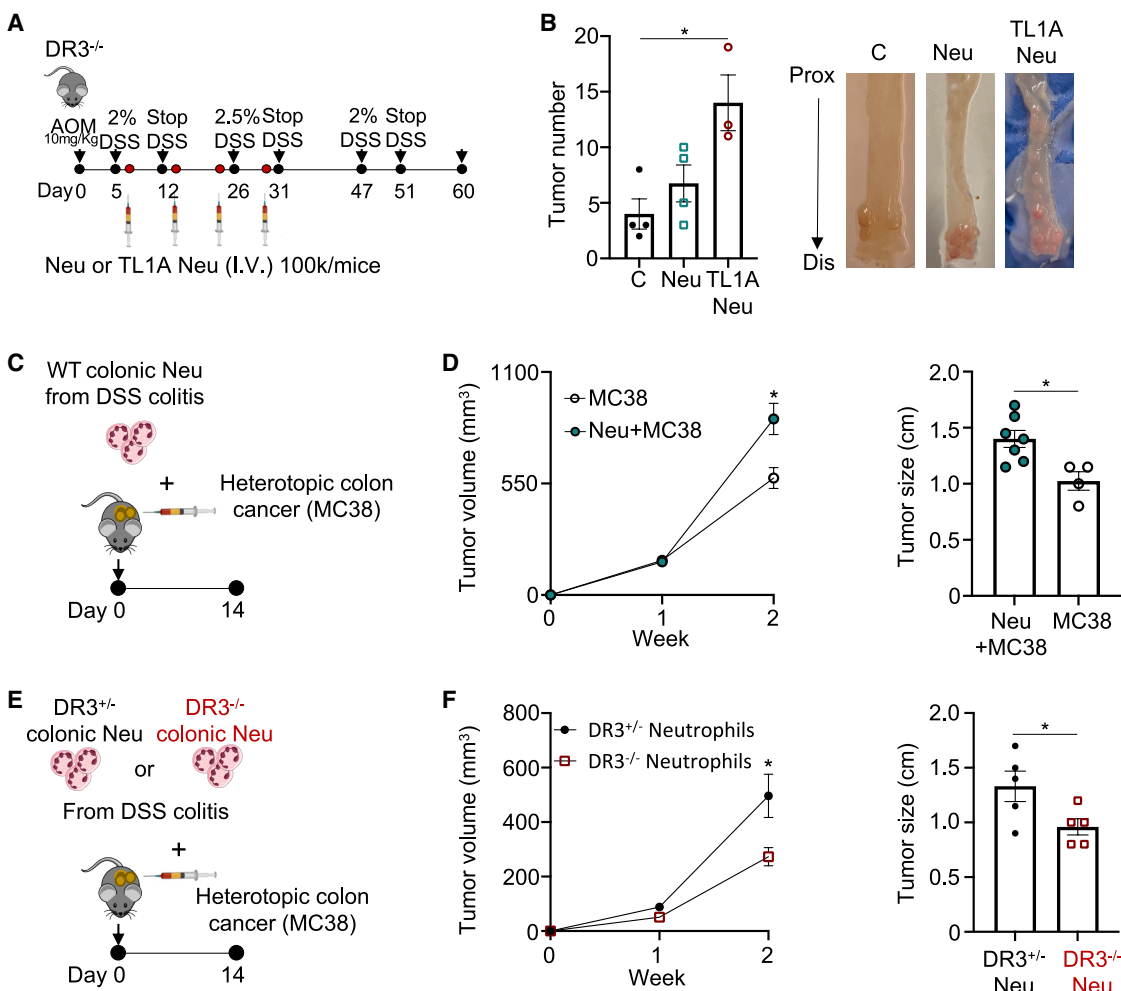


Figure 4. TL1A-stimulated ILC3s activate neutrophils that are sufficient to promote tumor growth

(A and B) $Rag1^{-/-}$ $DR3^{-/-}$ mice subjected to AOM/DSS received bone-marrow-derived neutrophils, stimulated or not with ILC3s supernatants following TL1A stimulation. (A) Schematic of the experimental approach used in (B). Neutrophils were activated *in vitro* using supernatants from intestinal ILC3s, stimulated with or without TL1A. 1×10^5 unstimulated neutrophils (Neu) or TL1A-activated neutrophils (TL1A Neu) were injected intravenously into $Rag1^{-/-}$ $DR3^{-/-}$ mice every 7 days, starting at day 2 of DSS for 4 weeks. (B) Tumor counts in the colons of $Rag1^{-/-}$ $DR3^{-/-}$ mice. One representative experiment out of two performed is shown (control $n = 4$; Neu $n = 4$; TL1A Neu $n = 3$). Representative images of colonic tumors at the AOM/DSS endpoint. (C and D) Mice were injected subcutaneously with either MC38 alone or MC38 and colonic neutrophils sorted from WT mice following DSS-induced colitis. (C) Schematic of the experimental approach used in D. (D) Tumor volume and size in mice injected with MC38 cells alone or co-injected with MC38 and colonic neutrophils. One representative experiment out of two performed is shown (MC38 $n = 4$; MC38 and Neutrophils $n = 7$). (E and F) Mice were injected subcutaneously with either MC38 alone or MC38 and colonic neutrophils sorted from $DR3^{+/−}$ (Het) or $DR3^{-/-}$ (KO) $Rag1^{-/-}$ mice following DSS-induced colitis. (E) Schematic of the experimental approach used in F. (F) Tumor volume and size in mice co-injected with MC38 cells and DR3 Het or KO neutrophils. Two pooled independent experiments (Het $n = 5$; KO $n = 5$).

Each dot represents an individual mouse. Data are presented as mean \pm standard error of the mean (SEM), and asterisks denote statistical significance (* $p < 0.05$). Statistical analyses were performed using unpaired Student's *t* tests (D and F) or one-way ANOVA with multiple comparisons (B).

See also Figure S3.

functional link between TL1A and colitis-associated granulopoiesis in humans.

ILC3 production of GM-CSF promotes emergency granulopoiesis

To determine whether TL1A drives emergency granulopoiesis by facilitating migration of tissue-resident ILC3s to the bone marrow, we used mice expressing a Kikume Green-Red (KikGR) reporter to track cellular migration from the colon to the bone marrow, as previously described.^{58,59} KikGR mice

were treated with either agonistic anti-DR3 or isotype control, followed by localized UV exposure to the colon to enable tracking of cell migration from the intestine (Figure S6A). Although agonistic anti-DR3 treatment induced expansion of bone marrow neutrophils (Figure S6B), no differences in the number or frequency of photoconverted (Red⁺) cells nor migration of CD90⁺ lymphocytes to the bone marrow were observed between groups (Figures S6C and S6D), suggesting that TL1A does not promote ILC3 migration to the bone marrow.

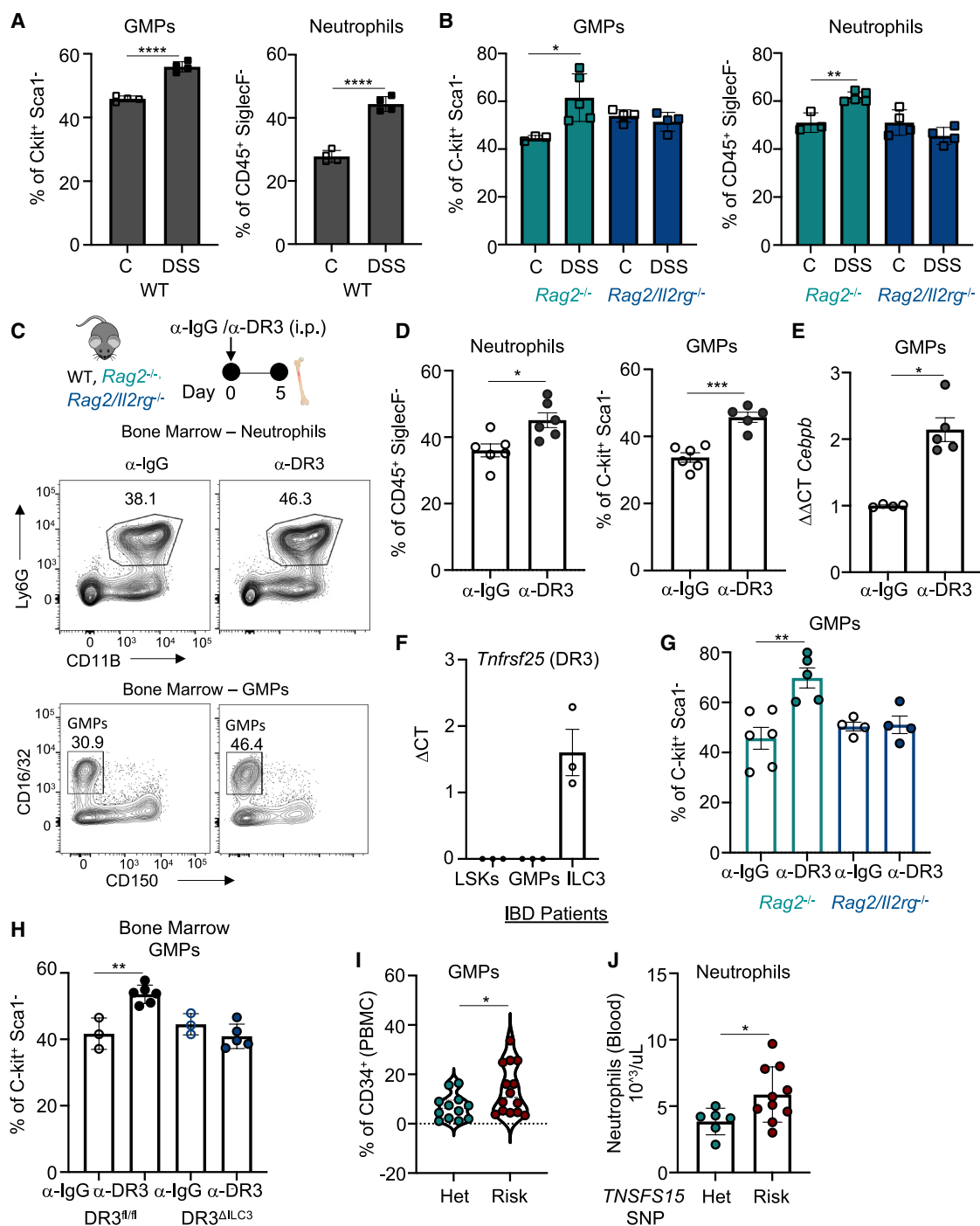


Figure 5. TL1A and colitis induce ILC3-mediated emergency granulopoiesis

(A and B) WT, *Rag2^{-/-}*, and *Rag2/Il2rg^{-/-}* mice were treated with water (control) or DSS for 6 days and analyzed at day 9. (A) Frequency of granulocyte-monocyte progenitors GMPs (gated as live, Lin⁻ Sca-1⁻ c-Kit⁺ CD150⁻ CD16/32⁺) and neutrophils (gated as live, CD45⁺ SiglecF⁻ CD11b⁺ Ly6G⁻) in the bone marrow of WT mice. One representative experiment out of two performed is shown (control n = 4, DSS n = 4). (B) Frequencies of GMPs and neutrophils in *Rag2^{-/-}* and *Rag2^{-/-}/Il2rg^{-/-}* mice one representative experiment out of two performed is shown (*Rag2^{-/-}*: control n = 3, DSS n = 5; *Rag2^{-/-}/Il2rg^{-/-}*: control n = 4, DSS n = 4). (C–G) Mice were treated with agonistic α -DR3 or isotype control. (C) Schematic of the experimental approach used in (C)–(G) and representative flow cytometry plots showing GMPs and neutrophils in the bone marrow of WT mice after treatment. (D) Frequencies of bone marrow GMPs and neutrophils in WT mice following treatment. One representative experiment out of two performed is shown (α -IgG n = 6, α -DR3 n = 6). (E) Expression of *Cebpb* in sorted GMPs (live, Lin⁻ Sca-1⁻ c-Kit⁺ CD150⁻ CD16/32⁺ CD34⁺) from the bone marrow of WT mice 1 day after treatment. Two pooled independent experiments (α -IgG n = 4, α -DR3 n = 5). (F) Expression of *Tnfrsf25* in sorted bone marrow LSKs (live, Lin⁻ Sca-1⁺ c-Kit⁺), GMPs, and intestinal ILC3s (n = 3 per group). (G) Frequencies of C-kit⁺ Sca1⁻ GMPs in IBD patients. (H) Frequencies of C-kit⁺ Sca1⁻ GMPs in DR3^{fl/fl} and DR3^{ΔILC3} mice. (I) Frequencies of CD34⁺ PBMCs in GMPs from Het and Risk individuals. (J) Neutrophils in blood from Het and Risk individuals. (TNSFS15 SNP)

(legend continued on next page)

To test the alternative hypothesis that TL1A drives ILC3 production of a diffusible serum factor that acts systemically to initiate emergency granulopoiesis, we stimulated sorted LSKs and GMPs from naive WT mice with serum collected 1 day after agonistic anti-DR3 or isotype control injection (Figure 6A). Serum from agonistic anti-DR3-treated mice induced increased expression of *Cebpb* and decreased expression of *Cebpa* in both progenitor populations (Figures 6B and S6E), consistent with a TL1A-induced serum soluble factor driving transcriptional changes characteristic of emergency granulopoiesis.

GM-CSF is a critical regulator of hematopoietic progenitor expansion and granulopoiesis.²² Although intestinal ILC3s are a major source of GM-CSF in UC,²⁷ the systemic impact of this GM-CSF production has not been investigated. Treatment with agonistic anti-DR3 induces GM-CSF production by colonic ILC3s, but not by T cells (Figures 6C and S6F), and results in elevated GM-CSF levels in both serum and bone marrow extracellular fluid (Figures 6D and 6E). Both interleukin (IL)-1 β and IL-6 have also been shown to impact and promote expansion of progenitors in the bone marrow.⁶⁰ Although modest increases in IL-6 were also detected in the serum, no changes in IL-1 β or bone marrow IL-6 were observed, suggesting a predominant role for GM-CSF in mediating the TL1A response (Figures 6D and 6E).

To directly test whether ILC3-derived GM-CSF mediates TL1A-dependent emergency granulopoiesis, we generated *Rorc-Cre Csf2^{f/f}* mice (referred to as *Csf2^{ΔRorc}*), which lack GM-CSF expression in ILC3s and T cells (Figure S6G). Compared with *Csf2^{f/f}* littermates, *Csf2^{ΔRorc}* mice exhibited significantly reduced serum GM-CSF following agonistic anti-DR3 (Figure 6F). In the bone marrow, TL1A-induced expansion of GMPs and neutrophils was abrogated in *Csf2^{ΔRorc}* mice (Figures 6G and 6H), supporting a critical function for ILC3-derived GM-CSF in promoting emergency granulopoiesis.

ILC3-derived GM-CSF drives neutrophil activation and tumorigenesis

As major producers of GM-CSF, ILC3s can help shape myeloid cell activation in the colon.^{61,62} To determine whether ILC3-derived GM-CSF directly regulates neutrophil activation, we first used our *in vitro* co-culture assay. Cytokine analysis of ILC3 supernatants following TL1A stimulation revealed elevated levels of GM-CSF (Figure S7A). Neutralization of GM-CSF, but not other cytokines produced by ILC3s, including IL-17 or IL-22, abrogated neutrophil activation induced by TL1A-stimulated ILC3s (Figure S7B). Similarly, ILC3s from *Csf2^{ΔRorc}* mice failed to induce neutrophil activation and expression of TAN markers—including CD14, PD-L1, and Siglec-F—when stimulated with TL1A, unlike control ILC3s (Figures 7A and S7C). To further

assess the impact *in vivo*, *Csf2^{ΔRorc}* were exposed to DSS. Despite similar levels of inflammation assessed by histology following DSS-induced colitis (Figure S7D), these mice displayed a marked reduction in colonic neutrophil infiltration and CD14 expression (Figures 7B and 7C). Furthermore, neutrophils from *Csf2^{ΔRorc}* mice showed diminished reactive oxygen species (ROS) production—an established driver of tumorigenesis—compared with heterozygous littermate controls (Figure 7C), aligning with previous reports linking GM-CSF to ROS induction in neutrophils.⁶³

To determine the role of ILC3-derived GM-CSF in CAC, we subjected *Csf2^{ΔRorc}* and *Csf2^{ΔILC3}* (*Rorc-Cre Csf2^{f/f}* on a *Rag2^{-/-}* background) mice, along with littermate controls, to AOM/DSS treatment. Deletion of GM-CSF in *Rorc-Cre Csf2^{f/f}* *Rag2^{-/-}* (*Csf2^{ΔILC3}*) mice was specific to ILC3s, as no impact was observed on GM-CSF production by ILC2s (Figure S7E). Following AOM/DSS, both *Csf2^{ΔILC3}* and *Csf2^{ΔRorc}* showed a significant reduction in tumor burden compared with controls (Figures 7D and 7E). To functionally assess the tumor-promoting capacity of colonic neutrophils induced by GM-CSF *in vivo*, colonic neutrophils were sorted from *Csf2^{f/f}* and *Csf2^{ΔRorc}* following colitis induction with DSS and co-injected with the CRC line MC38 to assess heterotopic growth (Figure 7F). Neutrophils from *Csf2^{ΔRorc}* mice failed to promote heterotopic tumor growth compared with those from controls (Figure 7G), supporting the role of ILC3-derived GM-CSF in driving tumor-promoting neutrophil activity *in vivo*. Notably, bone-marrow-derived neutrophils from colitic mice were also not sufficient to enhance tumor growth (Figure S7F), highlighting the importance of the colonic microenvironment in neutrophil adaptation and pro-tumor function. Collectively, these findings reveal a unique role for TL1A-induced GM-CSF from intestinal tissue-resident ILC3s in orchestrating systemic emergency granulopoiesis and promoting a population of tumor-promoting neutrophils critical for CAC development.

DISCUSSION

TL1A can have dual effects: it may help limit inflammation during acute colitis but exacerbate pathology during chronic inflammation.^{11,64,65} Consistent with this notion, TL1A overexpression in mouse models promotes CAC.¹⁵ Here, we identified colonic tissue-resident ILC3s as key sensors of TL1A signaling, essential for promoting CAC during chronic models of inflammation. TL1A-stimulated ILC3s activated neutrophils and drove expression of genes associated with neutrophils presents in tumors. Furthermore, TL1A mediated neutrophil recruitment and activation in the colon, which was sufficient to promote CAC. Neutrophil accumulation occurred near neoplastic epithelial cells,

(G) Frequency of GMPs in the bone marrow of *Rag2^{-/-}* (α -IgG n = 6, α -DR3 n = 5) and *Rag2^{-/-}/I2rg^{-/-}* mice (α -IgG n = 4, α -DR3 n = 4), 5 days after treatment. One representative experiment out of three performed is shown (*Rag2^{-/-}*: α -IgG n = 6, α -DR3 n = 5; *Rag2^{-/-}/I2rg^{-/-}*: α -IgG n = 4, α -DR3 n = 4).

(H) Frequency of GMPs in *Tnfrsf25^{f/f}* (Hets) and *Rorc Cre Tnfrsf25^{f/f}* (KO) *Rag2^{-/-}* mice 5 days after treatment with α -DR3 or isotype control. One representative experiment out of two performed is shown (Het: α -IgG n = 3, α -DR3 n = 6; KO: α -IgG n = 3, α -DR3 n = 4).

(I) Frequency of circulating GMPs (live, Lin $^-$ CD34 $^+$ CD38 $^+$ CD45RA $^+$) in the blood of IBD patients with *TNFSF15* SNPs (Het n = 12; Risk n = 14).

(J) Counts of circulating neutrophils in the blood of IBD subjects carrying heterozygous or risk *TNFSF15* SNPs (Het n = 6; Risk n = 10).

Each dot represents an individual mouse or human subject. Results are presented as mean \pm standard error of the mean (SEM), and asterisks denote statistical significance (*p < 0.05, **p < 0.01, ***p < 0.001, ****p < 0.0001). Statistical analyses were performed using unpaired Student's t tests (A, D, E, I, and J) or one-way ANOVA with multiple comparisons (B, G, and H).

See also Figures S4 and S5.

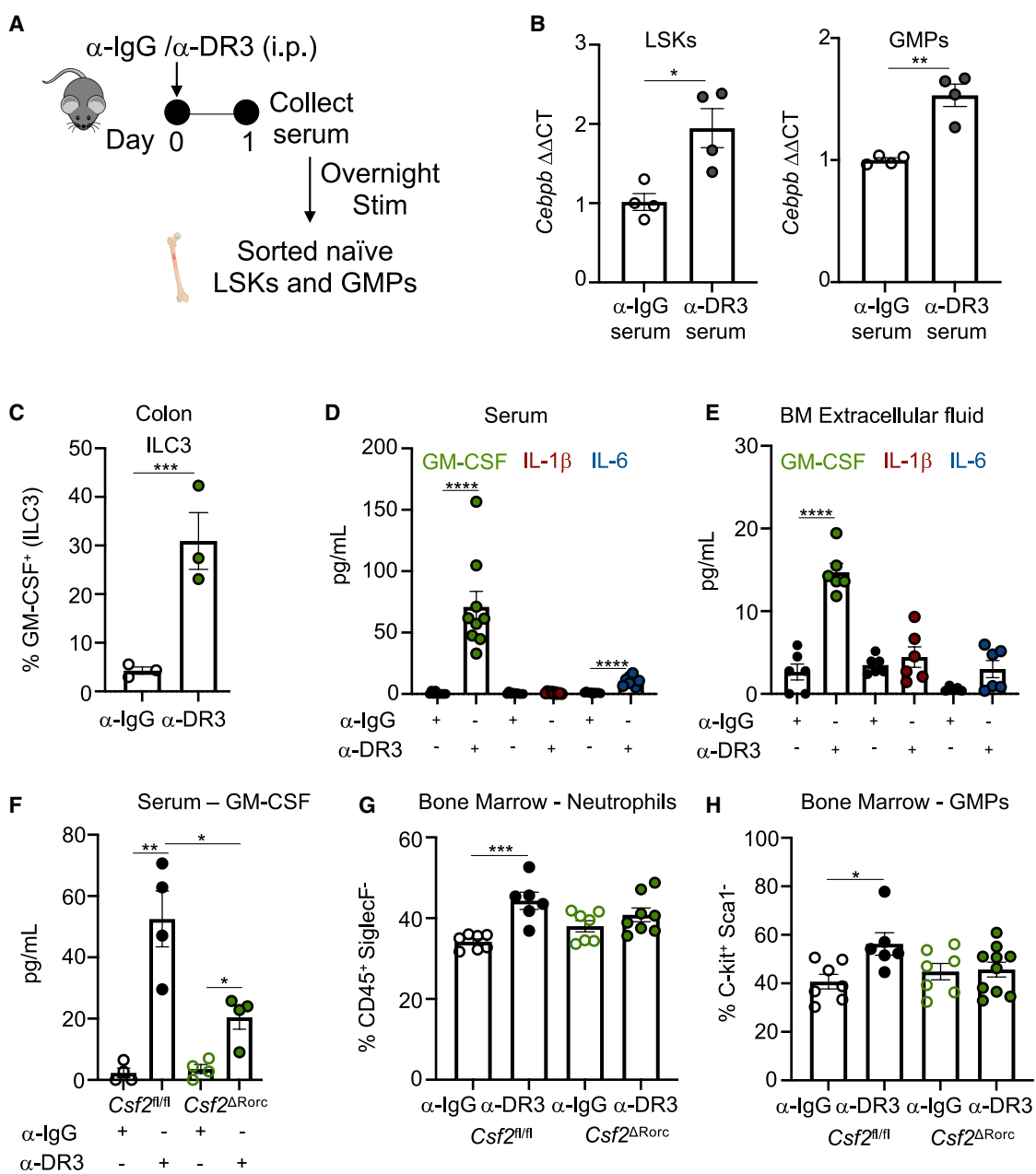


Figure 6. ILC3-derived GM-CSF is required for TL1A-mediated emergency granulopoiesis

(A–E) WT mice were treated with isotype control or agonistic α -DR3. (A) Schematic of the experimental approach used in B. (B) Expression of *Cebpb* in LSKs and GMPs after serum stimulation. Two pooled independent experiments (serum α -IgG $n = 4$, serum α -DR3 $n = 4$). (C) Frequency of GM-CSF⁺ colonic ILC3s following treatment. One representative experiment out of three performed is shown (α -IgG $n = 3$, α -DR3 $n = 3$). (D) GM-CSF levels in serum 1 day post-treatment. Three pooled independent experiments (α -IgG $n = 9$, α -DR3 $n = 9$). (E) GM-CSF levels in bone marrow extracellular fluid 1 day post-treatment. Two pooled independent experiments (α -IgG $n = 6$, α -DR3 $n = 6$).

(F–H) *Csf2^{fl/fl}* (Hets) and *Rorc Cre⁺ Csf2^{fl/fl}* (KO) mice treated with isotype control or α DR3. (F) GM-CSF levels in serum 1 day post-treatment. One representative experiment out of two performed is shown (Het α -IgG $n = 4$, α -DR3 $n = 4$; KO α -IgG $n = 4$, α -DR3 $n = 4$). (G) Frequency of bone marrow neutrophils 5 days post-treatment. Two pooled independent experiments (Het α -IgG $n = 7$, α -DR3 $n = 6$; KO α -IgG $n = 7$, α -DR3 $n = 8$). (H) Frequency of bone marrow GMPs 5 days post-treatment. Two pooled independent experiments (Het α -IgG $n = 7$, α -DR3 $n = 6$; KO α -IgG $n = 7$, α -DR3 $n = 9$). Each dot represents an individual mouse. Results are expressed as mean \pm standard error of the mean (SEM), and asterisks denote statistical significance (* $p < 0.05$, ** $p < 0.01$, *** $p < 0.001$, **** $p < 0.00001$). Statistical analyses were performed using unpaired Student's *t* tests (B and C) or one-way ANOVA with multiple comparisons (D–H).

See also Figure S6.

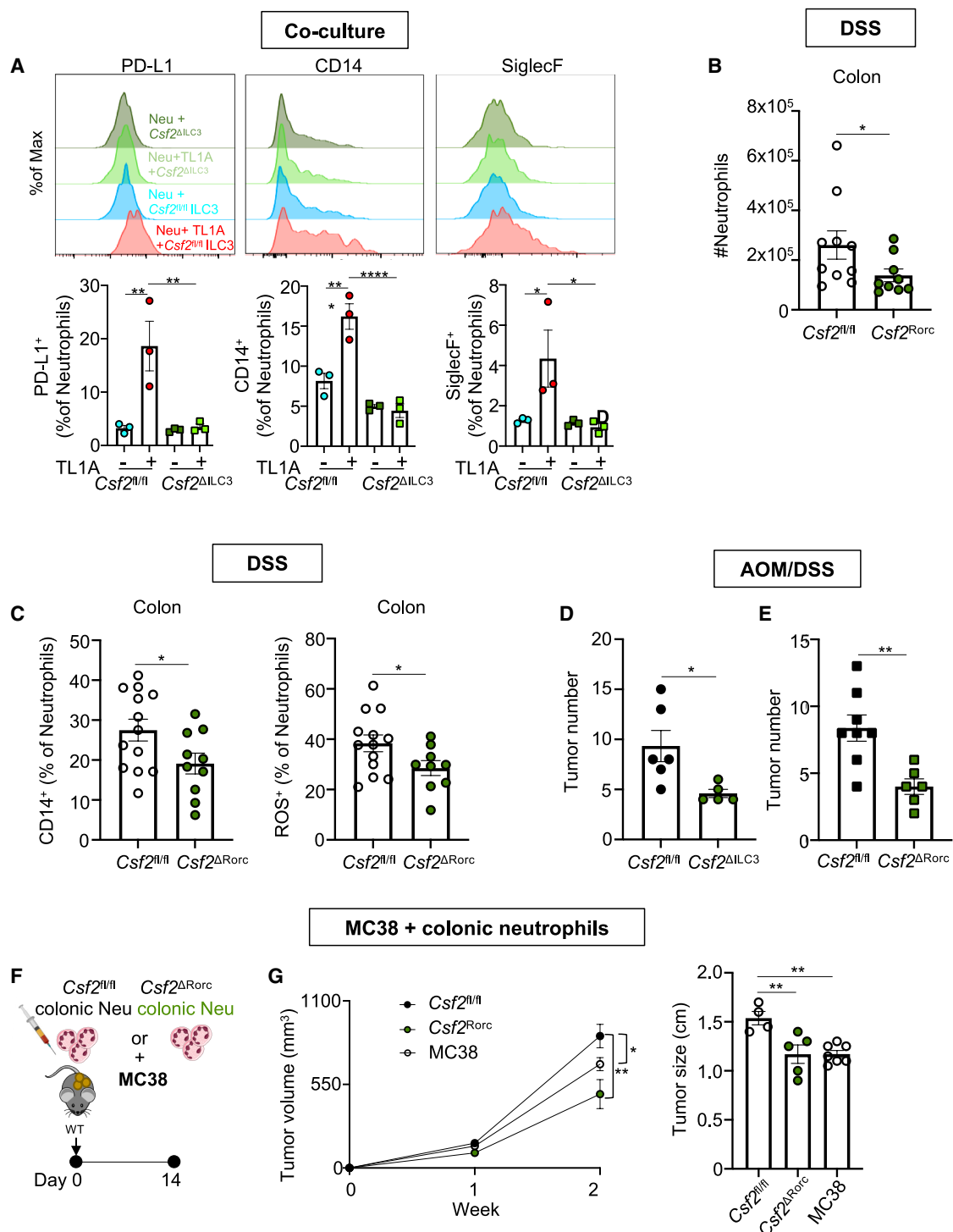


Figure 7. ILC3-derived GM-CSF is required for TL1A-mediated colitis-associated tumorigenesis

(A) Representative histograms and quantification of PD-L1⁺, CD14⁺, and SiglecF⁺ neutrophils following *in vitro* co-culture with intestinal ILC3s from Csf2^{ΔRorc} (KO) or heterozygous littermate controls (Het). One representative experiment out of three performed is shown.

(B and C) Csf2^{f/f} (Het) and Csf2^{ΔRorc} (KO) mice were treated with DSS for 6 days and analyzed 2 days after DSS cessation. (B) Total number of colonic neutrophils. Three pooled independent experiments (Het $n = 10$, KO $n = 9$). (C) Frequency of CD14⁺ colonic neutrophils and ROS⁺ colonic neutrophils. Three pooled independent experiments (Het $n = 7$, KO $n = 10$).

(D) Number of colonic tumors in Csf2^{f/f} (Hets) and Rorc Cre Csf2^{f/f} (KO) Rag2^{-/-} mice. Two pooled independent experiments (Het $n = 7$, KO, $n = 6$).

(E) Number of colonic tumors in Csf2^{f/f} (Hets) and Rorc Cre Csf2^{f/f} (KO) mice. Two pooled independent experiments (Het $n = 8$, KO, $n = 6$).

(legend continued on next page)

providing evidence for spatial co-localization. These findings align with the identification of an epithelium-associated inflammatory neutrophil population enriched in the colons of individuals with IBD.⁴⁴ A role for ILC3s in tumor development and cancer is emerging. In addition to chronic IL-22 production driving epithelial hyperproliferation,⁶⁶ expression of major histocompatibility complex class II (MHCII) on ILC3 can dampen T cell immunity and the response to checkpoint inhibitors.⁶⁷ Our work reveals a role for ILC3s in cancer wherein they shape tissue adaptation of neutrophils that promote colitis-associated tumor development.

Neutrophil infiltration is linked to poor outcomes in both sporadic CRC and CAC.^{46,68} With growing appreciation for the heterogeneity of neutrophils in cancer and inflammation,^{17,69} emerging evidence highlights a specific transcriptional program in TANs during colitis-driven tumorigenesis. This includes established TAN markers (*Cd14*, *Cd9*, and *Runx1*), transcription factors (*Irf5*, *RelB*, and *NfkB1/2*), and pro-angiogenic genes that support tumor vascularization.⁴⁴ We found that TL1A-activated ILC3s induced this TAN gene signature in neutrophils, including inflammatory mediators *Il1b* and *Ptgs2*, which are elevated in IBD and implicated in CAC development.^{45–48} Functionally, TL1A signaling *in vivo* drove expression of these TAN markers in colonic neutrophils and adoptive transfer of TL1A-activated neutrophils was sufficient to enhance tumorigenesis. Although TL1A can induce expression of functional markers of TANs *in situ* to promote tumorigenesis, multiple factors, including timing, may contribute to the pro-tumorigenic effect of neutrophils.^{40–42} Digital spatial profiling in both IBD-associated and non-IBD dysplastic colon tissue further highlights the specificity of these TAN markers in colitis-associated dysplasia, and the reduction in expression of these marker genes following TL1A blockade in UC supports a role for TL1A signaling in modulating TANs in humans. Given the emerging clinical trials of anti-TL1A therapies for moderate to severe UC,⁸ our findings support further investigation into their potential for preventing colitis-associated cancer.²⁵

Mechanistically, we found that TL1A signaling in tissue-resident ILC3s orchestrates two key aspects of the neutrophil response: emergency granulopoiesis and tissue adaptation.²⁰ Infection, inflammation, and cancer can all induce emergency granulopoiesis to meet increased peripheral demand for neutrophils. TL1A-activated ILC3s, through production of GM-CSF, drove this process during colonic inflammation. Notably, GM-CSF-neutralizing antibodies are detected years before the onset of Crohn's disease, suggesting episodic systemic GM-CSF exposure may be immunogenic and involved in disease progression.⁷⁰ The intestinal microbiota and microbial translocation can also promote granulopoiesis during colitis.^{71–73} Microbial regulation of TL1A may provide a mechanistic link between dysbiosis and tissue-resident immune responses with systemic effects.

Interestingly, neutrophils from the bone marrow of colitic mice did not promote tumor growth, underscoring the importance of tissue adaptation in conferring tumor-promoting capacity. ILC3-derived GM-CSF was required for the accumulation of neutrophils in the colon, expression of TAN markers, and their capacity for supporting tumorigenesis. GM-CSF can act as a double-edged sword in mediating both intestinal healing and inflammation. ILC3-derived GM-CSF regulates myeloid cells and maintains intestinal homeostasis.^{61,70} Although early trials with recombinant GM-CSF (sargramostim) suggested symptom relief in Crohn's disease,⁷⁴ larger studies failed to show significant benefit,⁷⁵ likely reflecting a more nuanced effect of GM-CSF in intestinal immunity.

Altogether, our findings reveal a role for TL1A signaling in tissue-resident ILC3s, linking colitis with emergency granulopoiesis as well as shaping tissue adaptation of neutrophils capable of promoting tumor growth. With TL1A inhibitors entering clinical trials, these insights strengthen the rationale for evaluating anti-TL1A therapies as a strategy to reduce cancer risk in IBD.

Limitations of the study

This study uncovers a role for TL1A in generating neutrophils with a pro-tumorigenic transcriptional profile and the functional capacity to promote tumor growth; however, the precise mechanism by which neutrophils initiate and sustain tumor growth in the setting of colitis remains incompletely defined. Moreover, although we mechanistically demonstrate in pre-clinical models that TL1A-induced GM-CSF links colitis with emergency granulopoiesis, our human data show only an association of higher circulating neutrophils and GMPs in individuals with quiescent CD with risk variants in *TNFSF15*. Future work incorporating direct TL1A protein measurements in patient samples and analyses from clinical trials of UC patients treated with TL1A blockade will be essential to validate and extend these findings.

RESOURCE AVAILABILITY

Lead contact

Requests for further information and resources should be directed to the lead contact, Dr. Randy S. Longman (ral2006@med.cornell.edu).

Materials availability

All reagents generated in this study are available from the [lead contact](#) upon request.

Data and code availability

RNA-seq data were deposited at NCBI and spatial molecular imaging data at Zenodo. Accession numbers are listed in the [key resources table](#). This paper does not report new original codes. Any additional information required to re-analyze the data reported in this paper is available from the [lead contact](#) upon request.

(F and G) WT mice were injected subcutaneously with either MC38 alone or MC38 and colonic neutrophils sorted from *Csf2^{f1/f1}* (Het) or *Csf2^{ΔRorc}* (KO) mice following DSS-induced colitis. (F) Schematic of the experimental approach used in G. (G) Tumor volume was monitored for 2 weeks. Tumor size was assessed at the endpoint. Two pooled independent experiments (MC38 alone $n = 7$; MC38 + Het colonic neutrophils $n = 4$; MC38 + KO colonic neutrophils $n = 5$). Each dot represents an individual mouse (B–G). Data are shown as mean \pm standard error of the mean (SEM), and asterisks denote statistical significance (* $p < 0.05$, ** $p < 0.01$, *** $p < 0.0001$). Statistical analysis was performed using unpaired Student's *t* tests (B, C, D, and E) or two-way ANOVA with multiple comparisons (A and G).

See also [Figure S7](#).

ACKNOWLEDGMENTS

We would like to acknowledge members of the Longman Laboratory for helpful discussions. We would like to thank Gregory Sonnenberg for helpful comments and critical discussions. We would like to thank the Genomics Cores of Weill Cornell Medicine and Steven Josefowicz and Rachel Niec for helpful feedback on progenitor cell analysis.

This work was supported by grants from the Crohn's and Colitis Foundation 953817 (S.P.), NHRMC 1113577 and 1154235 (I.W.), the Reid Charitable Trusts (I.W.), R01 DK120985 (R.S.L.), and R01 DK128257 (R.S.L.). Funding was also provided by CURE for IBD and a generous gift from the Mishaan family.

AUTHOR CONTRIBUTIONS

S.P. and R.S.L. conceived the project and wrote the manuscript, with input from all authors. S.P. performed all the experiments and analyzed the data. W.Y., Y.L.Z., and A.C. provided experimental assistance. S.F. and J.G. performed and analyzed the spatial transcriptomics data. E.C., M.H.-Z., Y.L.Z., C.H., K.H., C.N., and A.G. contributed to data analysis. C.L., T.L.P., G.E.D., S.R.T., and I.W. provided essential tools and scientific expertise. N.T., D.L., E.S., and JRI Live Cell Bank contributed to clinical sample acquisition and processing. S.P., I.W., and R.S.L. acquired the funding.

DECLARATION OF INTERESTS

R.S.L. is a consultant for Pfizer and Sanofi, a special advisory board member of CJ Biosciences and Ancilia Biosciences, and a grant recipient of Boehringer Ingelheim. M.H.-Z., Y.L.Z., C.H., and K.H. are employees of Pfizer. S.R.T. is a stockholder and founder of and consultant for Prometheus Biosciences. D.L. is a consultant for Abbvie, Boehringer Ingelheim, BMS, Eli Lilly, Fresenius Kabi, Janssen, Palatin Technologies, Pfizer, and Prometheus Laboratories and receives grant support from Abbvie, Janssen, and Takeda.

STAR METHODS

Detailed methods are provided in the online version of this paper and include the following:

KEY RESOURCES TABLE

EXPERIMENTAL MODEL AND STUDY PARTICIPANT DETAILS

○ Human PBMCs

○ Digital spatial RNA profiling

○ Colitis and colorectal tumor models

METHOD DETAILS

○ Mice

○ Bone Marrow isolation of neutrophils

○ Murine intestinal immune cell isolation

○ Intestinal ILC isolation

○ Cell depletion

○ Flow cytometry staining and analyses

○ Co-culture assays

○ Cytokine quantification

○ Bone marrow progenitor isolation and ex vivo stimulation

○ Tracking of intestinal cell trafficking by photoconversion of KikGR33 mice

○ RNA-seq

○ CosMx spatial molecular imaging analysis pipeline

○ Neighborhood enrichment analysis

○ Gene expression by Quantitative RT-PCR

○ Histological analysis and colitis scoring

○ TNFSF15 SNP genotyping

○ Digital spatial RNA profiling

○ Statistical analysis

SUPPLEMENTAL INFORMATION

Supplemental information can be found online at <https://doi.org/10.1016/j.immuni.2025.12.008>.

Received: October 7, 2024

Revised: July 15, 2025

Accepted: December 11, 2025

REFERENCES

1. Herrinton, L.J., Liu, L., Levin, T.R., Allison, J.E., Lewis, J.D., and Velayos, F. (2012). Incidence and mortality of colorectal adenocarcinoma in persons with inflammatory bowel disease from 1998 to 2010. *Gastroenterology* 143, 382–389. <https://doi.org/10.1053/j.gastro.2012.04.054>.
2. Jess, T., Simonsen, J., Jørgensen, K.T., Pedersen, B.V., Nielsen, N.M., and Frisch, M. (2012). Decreasing risk of colorectal cancer in patients with inflammatory bowel disease over 30 years. *Gastroenterology* 143, 375–381.e1. <https://doi.org/10.1053/j.gastro.2012.04.016>.
3. Rubin, C.E., Haggitt, R.C., Burmer, G.C., Brentnall, T.A., Stevens, A.C., Levine, D.S., Dean, P.J., Kimmey, M., Perera, D.R., and Rabinovitch, P.S. (1992). DNA aneuploidy in colonic biopsies predicts future development of dysplasia in ulcerative colitis. *Gastroenterology* 103, 1611–1620. [https://doi.org/10.1016/0016-5085\(92\)91185-7](https://doi.org/10.1016/0016-5085(92)91185-7).
4. Axelrad, J.E., Lichtiger, S., and Yajnik, V. (2016). Inflammatory bowel disease and cancer: The role of inflammation, immunosuppression, and cancer treatment. *World J. Gastroenterol.* 22, 4794–4801. <https://doi.org/10.3748/wjg.v22.i20.4794>.
5. Bamias, G., Jia, L.G., and Cominelli, F. (2013). The tumor necrosis factor-like cytokine 1A/death receptor 3 cytokine system in intestinal inflammation. *Curr. Opin. Gastroenterol.* 29, 597–602. <https://doi.org/10.1097/MOG.0b013e328365d3a2>.
6. Siakavellas, S.I., Sfikakis, P.P., and Bamias, G. (2015). The TL1A/DR3/DcR3 pathway in autoimmune rheumatic diseases. *Semin. Arthritis Rheum.* 45, 1–8. <https://doi.org/10.1016/j.semarthrit.2015.02.007>.
7. Bamias, G., Menghini, P., Pizarro, T.T., and Cominelli, F. (2025). Targeting TL1A and DR3: the new frontier of anti-cytokine therapy in IBD. *Gut* 74, 652–668. <https://doi.org/10.1136/gutjnl-2024-332504>.
8. Michelsen, K.S., Thomas, L.S., Taylor, K.D., Yu, Q.T., Mei, L., Landers, C.J., Derkowski, C., McGovern, D.P.B., Rotter, J.I., and Targan, S.R. (2009). IBD-associated TL1A gene (TNFSF15) haplotypes determine increased expression of TL1A protein. *PLoS One* 4, e4719. <https://doi.org/10.1371/journal.pone.0004719>.
9. Shih, D.Q., Kwan, L.Y., Chavez, V., Cohavy, O., Gonsky, R., Chang, E.Y., Chang, C., Elson, C.O., and Targan, S.R. (2009). Microbial induction of inflammatory bowel disease associated gene TL1A (TNFSF15) in antigen presenting cells. *Eur. J. Immunol.* 39, 3239–3250. <https://doi.org/10.1002/eji.200839087>.
10. Richard, A.C., Peters, J.E., Savinykh, N., Lee, J.C., Hawley, E.T., Meylan, F., Siegel, R.M., Lyons, P.A., and Smith, K.G.C. (2018). Reduced monocyte and macrophage TNFSF15/TL1A expression is associated with susceptibility to inflammatory bowel disease. *PLoS Genet.* 14, e1007458. <https://doi.org/10.1371/journal.pgen.1007458>.
11. Castellanos, J.G., Woo, V., Viladomiu, M., Putzel, G., Lima, S., Diehl, G.E., Marderstein, A.R., Gandara, J., Perez, A.R., Withers, D.R., et al. (2018). Microbiota-Induced TNF-like Ligand 1A Drives Group 3 Innate Lymphoid Cell-Mediated Barrier Protection and Intestinal T Cell Activation during Colitis. *Immunity* 49, 1077–1089.e5. <https://doi.org/10.1016/j.immuni.2018.10.014>.
12. Meylan, F., Hawley, E.T., Barron, L., Barlow, J.L., Penumetcha, P., Pelletier, M., Sciumè, G., Richard, A.C., Hayes, E.T., Gomez-Rodriguez, J., et al. (2014). The TNF-family cytokine TL1A promotes allergic immunopathology through group 2 innate lymphoid cells. *Mucosal Immunol.* 7, 958–968. <https://doi.org/10.1038/mi.2013.114>.
13. Valatas, V., Kolios, G., and Bamias, G. (2019). TL1A (TNFSF15) and DR3 (TNFRSF25): A Co-stimulatory System of Cytokines With Diverse Functions in Gut Mucosal Immunity. *Front. Immunol.* 10, 583. <https://doi.org/10.3389/fimmu.2019.00583>.

14. Hedi, M., and Abraham, C. (2014). A TNFSF15 disease-risk polymorphism increases pattern-recognition receptor-induced signaling through caspase-8-induced IL-1. *Proc. Natl. Acad. Sci. USA* 111, 13451–13456. <https://doi.org/10.1073/pnas.1404178111>.
15. Niu, W., Wu, Z., Wang, J., Zhang, H., Jia, W., Yang, M., Luo, Y., and Zhang, X. (2018). Tumor Necrosis Factor Ligand-Related Molecule 1A Regulates the Occurrence of Colitis-Associated Colorectal Cancer. *Dig. Dis. Sci.* 63, 2341–2350. <https://doi.org/10.1007/s10620-018-5126-0>.
16. Ślebioda, T.J., Stanisławowski, M., Cyman, M., Wierzbicki, P.M., Żurawka-Janicka, D., Kobiela, J., Makarewicz, W., Guzek, M., and Kmiec, Z. (2019). Distinct Expression Patterns of Two Tumor Necrosis Factor Superfamily Member 15 Gene Isoforms in Human Colon Cancer. *Dig. Dis. Sci.* 64, 1857–1867. <https://doi.org/10.1007/s10620-019-05507-8>.
17. Ng, L.G., Ostuni, R., and Hidalgo, A. (2019). Heterogeneity of neutrophils. *Nat. Rev. Immunol.* 19, 255–265. <https://doi.org/10.1038/s41577-019-0141-8>.
18. Garrido-Trigo, A., Corraliza, A.M., Veny, M., Dotti, I., Melón-Ardanaz, E., Rill, A., Crowell, H.L., Corbí, Á., Gudiño, V., Esteller, M., et al. (2023). Macrophage and neutrophil heterogeneity at single-cell spatial resolution in human inflammatory bowel disease. *Nat. Commun.* 14, 4506. <https://doi.org/10.1038/s41467-023-40156-6>.
19. Yalom, L.K., Herrnreiter, C.J., Bui, T.M., Lockhart, J., Piccolo, E.B., Ren, X., Wei, C., Serdiukova, A., Thorp, E.B., Dulai, P.S., et al. (2025). Spatially separated epithelium-associated and lamina propria neutrophils present distinct functional identities in the inflamed colon mucosa. *Mucosal Immunol.* 18, 685–699. <https://doi.org/10.1016/j.mucimm.2025.02.008>.
20. Ng, M., Cerezo-Wallis, D., Ng, L.G., and Hidalgo, A. (2025). Adaptations of neutrophils in cancer. *Immunity* 58, 40–58. <https://doi.org/10.1016/j.immuni.2024.12.009>.
21. Quail, D.F., Amulic, B., Aziz, M., Barnes, B.J., Eruslanov, E., Fridlender, Z.G., Goodridge, H.S., Granot, Z., Hidalgo, A., Huttenlocher, A., et al. (2022). Neutrophil phenotypes and functions in cancer: A consensus statement. *J. Exp. Med.* 219, e20220011. <https://doi.org/10.1084/jem.20220011>.
22. Manz, M.G., and Boettcher, S. (2014). Emergency granulopoiesis. *Nat. Rev. Immunol.* 14, 302–314. <https://doi.org/10.1038/nri3660>.
23. Coffelt, S.B., Wellenstein, M.D., and de Visser, K.E. (2016). Neutrophils in cancer: neutral no more. *Nat. Rev. Cancer* 16, 431–446. <https://doi.org/10.1038/nrc.2016.52>.
24. Kugathasan, S., Baldassano, R.N., Bradfield, J.P., Sleiman, P.M.A., Imielinski, M., Guthery, S.L., Cucchiara, S., Kim, C.E., Frackleton, E.C., Annaiah, K., et al. (2008). Loci on 20q13 and 21q22 are associated with pediatric-onset inflammatory bowel disease. *Nat. Genet.* 40, 1211–1215. <https://doi.org/10.1038/ng.203>.
25. Danese, S., Klopocka, M., Scherl, E.J., Romatowski, J., Allegretti, J.R., Peeva, E., Vincent, M.S., Schoenbeck, U., Ye, Z., Hassan-Zahraee, M., et al. (2021). Anti-TL1A Antibody PF-06480605 Safety and Efficacy for Ulcerative Colitis: A Phase 2a Single-Arm Study. *Clin. Gastroenterol. Hepatol.* 19, 2324–2332.e6. <https://doi.org/10.1016/j.cgh.2021.06.011>.
26. Sands, B.E., Feagan, B.G., Peyrin-Biroulet, L., Danese, S., Rubin, D.T., Laurent, O., Luo, A., Nguyen, D.D., Lu, J., Yen, M., et al. (2024). Phase 2 Trial of Anti-TL1A Monoclonal Antibody Tulisokibart for Ulcerative Colitis. *N. Engl. J. Med.* 391, 1119–1129. <https://doi.org/10.1056/NEJMoa2314076>.
27. Martin, J.C., Chang, C., Boschetti, G., Ungaro, R., Giri, M., Grout, J.A., Gettler, K., Chuang, L.S., Nayar, S., Greenstein, A.J., et al. (2019). Single-Cell Analysis of Crohn's Disease Lesions Identifies a Pathogenic Cellular Module Associated with Resistance to Anti-TNF Therapy. *Cell* 178, 1493–1508.e20. <https://doi.org/10.1016/j.cell.2019.08.008>.
28. Smillie, C.S., Biton, M., Ordovas-Montanes, J., Sullivan, K.M., Burgin, G., Graham, D.B., Herbst, R.H., Rogel, N., Slyper, M., Waldman, J., et al. (2019). Intra- and Inter-cellular Rewiring of the Human Colon during Ulcerative Colitis. *Cell* 178, 714–730.e22. <https://doi.org/10.1016/j.cell.2019.06.029>.
29. Okayasu, I., Ohkusa, T., Kajiura, K., Kanno, J., and Sakamoto, S. (1996). Promotion of colorectal neoplasia in experimental murine ulcerative colitis. *Gut* 39, 87–92. <https://doi.org/10.1136/gut.39.1.87>.
30. Greten, F.R., Eckmann, L., Greten, T.F., Park, J.M., Li, Z.W., Egan, L.J., Kagnoff, M.F., and Karin, M. (2004). IKKbeta links inflammation and tumorigenesis in a mouse model of colitis-associated cancer. *Cell* 118, 285–296. <https://doi.org/10.1016/j.cell.2004.07.013>.
31. Yu, X., Pappu, R., Ramirez-Carrozzi, V., Ota, N., Caplazi, P., Zhang, J., Yan, D., Xu, M., Lee, W.P., and Grogan, J.L. (2014). TNF superfamily member TL1A elicits type 2 innate lymphoid cells at mucosal barriers. *Mucosal Immunol.* 7, 730–740. <https://doi.org/10.1038/mi.2013.92>.
32. Bamias, G., Filidou, E., Goukos, D., Valatas, V., Arvanitidis, K., Panagopoulou, M., Kouklakis, G., Daikos, G.L., Ladas, S.D., and Kolios, G. (2017). Crohn's disease-associated mucosal factors regulate the expression of TNF-like cytokine 1A and its receptors in primary subepithelial intestinal myofibroblasts and intestinal epithelial cells. *Transl. Res.* 180, 118–130.e2. <https://doi.org/10.1016/j.trsl.2016.08.007>.
33. Shimodaira, Y., More, S.K., Hamade, H., Blackwood, A.Y., Abraham, J.P., Thomas, L.S., Miller, J.H., Stamps, D.T., Castanon, S.L., Jacob, N., et al. (2023). DR3 Regulates Intestinal Epithelial Homeostasis and Regeneration After Intestinal Barrier Injury. *Cell. Mol. Gastroenterol. Hepatol.* 16, 83–105. <https://doi.org/10.1016/j.jcmgh.2023.03.008>.
34. Longman, R.S., Diehl, G.E., Victorio, D.A., Huh, J.R., Galan, C., Miraldi, E.R., Swaminath, A., Bonneau, R., Scherl, E.J., and Littman, D.R. (2014). CX(3)CR1(+) mononuclear phagocytes support colitis-associated innate lymphoid cell production of IL-22. *J. Exp. Med.* 211, 1571–1583. <https://doi.org/10.1084/jem.20140678>.
35. Ahn, Y.O., Weeres, M.A., Neulen, M.L., Choi, J., Kang, S.H., Heo, D.S., Bergerson, R., Blazar, B.R., Miller, J.S., and Verneris, M.R. (2015). Human group3 innate lymphoid cells express DR3 and respond to TL1A with enhanced IL-22 production and IL-2-dependent proliferation. *Eur. J. Immunol.* 45, 2335–2342. <https://doi.org/10.1002/eji.201445213>.
36. Singel, K.L., and Segal, B.H. (2016). Neutrophils in the tumor microenvironment: trying to heal the wound that cannot heal. *Immunol. Rev.* 273, 329–343. <https://doi.org/10.1111/imr.12459>.
37. Kim, B.S., Nishikii, H., Baker, J., Pierini, A., Schneidawind, D., Pan, Y., Beilhack, A., Park, C.G., and Negrin, R.S. (2015). Treatment with agonistic DR3 antibody results in expansion of donor Tregs and reduced graft-versus-host disease. *Blood* 126, 546–557. <https://doi.org/10.1182/blood-2015-04-637587>.
38. Shaul, M.E., and Fridlender, Z.G. (2019). Tumour-associated neutrophils in patients with cancer. *Nat. Rev. Clin. Oncol.* 16, 601–620. <https://doi.org/10.1038/s41571-019-0222-4>.
39. Hedrick, C.C., and Malanchi, I. (2022). Neutrophils in cancer: heterogeneous and multifaceted. *Nat. Rev. Immunol.* 22, 173–187. <https://doi.org/10.1038/s41577-021-00571-6>.
40. Veglia, F., Hashimoto, A., Dweep, H., Sansevieri, E., De Leo, A., Tcyganov, E., Kossenkov, A., Mulligan, C., Nam, B., Masters, G., et al. (2021). Analysis of classical neutrophils and polymorphonuclear myeloid-derived suppressor cells in cancer patients and tumor-bearing mice. *J. Exp. Med.* 218, e20201803. <https://doi.org/10.1084/jem.20201803>.
41. Engblom, C., Pfirschke, C., Zilionis, R., Da Silva Martins, J., Bos, S.A., Courtney, G., Rickelt, S., Severe, N., Baryawno, N., Faget, J., et al. (2017). Osteoblasts remotely supply lung tumors with cancer-promoting SiglecHigh neutrophils. *Science* 358, eaal5081. <https://doi.org/10.1126/science.aal5081>.
42. Gungabeesoon, J., Gort-Freitas, N.A., Kiss, M., Bolli, E., Messemaker, M., Siwicki, M., Hicham, M., Bill, R., Koch, P., Cianciaruso, C., et al. (2023). A neutrophil response linked to tumor control in immunotherapy. *Cell* 186, 1448–1464.e20. <https://doi.org/10.1016/j.cell.2023.02.032>.
43. Marigo, I., Bosio, E., Solito, S., Mesa, C., Fernandez, A., Dolcetti, L., Ugel, S., Sonda, N., Bicciato, S., Falisi, E., et al. (2010). Tumor-induced tolerance and immune suppression depend on the C/EBPbeta transcription

- factor. *Immunity* 32, 790–802. <https://doi.org/10.1016/j.jimmuni.2010.05.010>.
44. Bui, T.M., Yalom, L.K., Ning, E., Urbanczyk, J.M., Ren, X., Herrnreiter, C.J., Disario, J.A., Wray, B., Schipma, M.J., Velichko, Y.S., et al. (2024). Tissue-specific reprogramming leads to angiogenic neutrophil specialization and tumor vascularization in colorectal cancer. *J. Clin. Investig.* 134, e174545. <https://doi.org/10.1172/JCI174545>.
45. Wang, D., and Dubois, R.N. (2010). The role of COX-2 in intestinal inflammation and colorectal cancer. *Oncogene* 29, 781–788. <https://doi.org/10.1038/onc.2009.421>.
46. Wang, Y., Wang, K., Han, G.C., Wang, R.X., Xiao, H., Hou, C.M., Guo, R.F., Dou, Y., Shen, B.F., Li, Y., et al. (2014). Neutrophil infiltration favors colitis-associated tumorigenesis by activating the interleukin-1 (IL-1)/IL-6 axis. *Mucosal Immunol.* 7, 1106–1115. <https://doi.org/10.1038/mi.2013.126>.
47. Ma, X., Aoki, T., Tsuruyama, T., and Narumiya, S. (2015). Definition of Prostaglandin E2-EP2 Signals in the Colon Tumor Microenvironment That Amplify Inflammation and Tumor Growth. *Cancer Res.* 75, 2822–2832. <https://doi.org/10.1158/0008-5472.CAN-15-0125>.
48. Aoki, T., and Narumiya, S. (2017). Prostaglandin E2-EP2 signaling as a node of chronic inflammation in the colon tumor microenvironment. *Inflamm. Regen.* 37, 4. <https://doi.org/10.1186/s41232-017-0036-7>.
49. Popivanova, B.K., Kostadinova, F.I., Furuichi, K., Shamekh, M.M., Kondo, T., Wada, T., Egashira, K., and Mukaida, N. (2009). Blockade of a chemo-kine, CCL2, reduces chronic colitis-associated carcinogenesis in mice. *Cancer Res.* 69, 7884–7892. <https://doi.org/10.1158/0008-5472.CAN-09-1451>.
50. Chun, E., Lavoie, S., Michaud, M., Gallini, C.A., Kim, J., Soucy, G., Odze, R., Glickman, J.N., and Garrett, W.S. (2015). CCL2 Promotes Colorectal Carcinogenesis by Enhancing Polymorphonuclear Myeloid-Derived Suppressor Cell Population and Function. *Cell Rep.* 12, 244–257. <https://doi.org/10.1016/j.celrep.2015.06.024>.
51. Khan, A.A., Alsahl, M.A., and Rahmani, A.H. (2018). Myeloperoxidase as an Active Disease Biomarker: Recent Biochemical and Pathological Perspectives. *Med. Sci. (Basel)* 6, 33. <https://doi.org/10.3390/medsci6020033>.
52. Hussain, S.P., Amstad, P., Raja, K., Ambs, S., Nagashima, M., Bennett, W.P., Shields, P.G., Ham, A.J., Swenberg, J.A., Marrogi, A.J., et al. (2000). Increased p53 mutation load in noncancerous colon tissue from ulcerative colitis: a cancer-prone chronic inflammatory disease. *Cancer Res.* 60, 3333–3337.
53. Trottier, M.D., Irwin, R., Li, Y., McCabe, L.R., and Fraker, P.J. (2012). Enhanced production of early lineages of monocytic and granulocytic cells in mice with colitis. *Proc. Natl. Acad. Sci. USA* 109, 16594–16599. <https://doi.org/10.1073/pnas.1213854109>.
54. Hirai, H., Zhang, P., Dayaram, T., Hetherington, C.J., Mizuno, S., Imanishi, J., Akashi, K., and Tenen, D.G. (2006). C/EBPbeta is required for 'emergency' granulopoiesis. *Nat. Immunol.* 7, 732–739. <https://doi.org/10.1038/ni1354>.
55. Tung, C.C., Wong, J.M., Lee, W.C., Liu, H.H., Chang, C.H., Chang, M.C., Chang, Y.T., Shieh, M.J., Wang, C.Y., and Wei, S.C. (2014). Combining TNFSF15 and ASCA IgA can be used as a predictor for the stenosis/perforating phenotype of Crohn's disease. *J. Gastroenterol. Hepatol.* 29, 723–729. <https://doi.org/10.1111/jgh.12496>.
56. Yang, D.H., Yang, S.K., Song, K., Hong, M., Park, S.H., Lee, H.S., Kim, J.B., Lee, H.J., Park, S.K., Jung, K.W., et al. (2014). TNFSF15 is an independent predictor for the development of Crohn's disease-related complications in Koreans. *J. Crohns Colitis* 8, 1315–1326. <https://doi.org/10.1016/j.crohns.2014.04.002>.
57. Cheong, J.G., Ravishankar, A., Sharma, S., Parkhurst, C.N., Grassmann, S.A., Wingert, C.K., Laurent, P., Ma, S., Paddock, L., Miranda, I.C., et al. (2023). Epigenetic memory of coronavirus infection in innate immune cells and their progenitors. *Cell* 186, 3882–3902.e24. <https://doi.org/10.1016/j.cell.2023.07.019>.
58. Nowotschin, S., and Hadjantonakis, A.K. (2009). Use of KikGR a photoconvertible green-to-red fluorescent protein for cell labeling and lineage analysis in ES cells and mouse embryos. *BMC Dev. Biol.* 9, 49. <https://doi.org/10.1186/1471-213X-9-49>.
59. Nakanishi, Y., Ikeuchi, R., Chtanova, T., Kusumoto, Y., Okuyama, H., Moriya, T., Honda, T., Kabashima, K., Watanabe, T., Sakai, Y., et al. (2018). Regulatory T cells with superior immunosuppressive capacity emigrate from the inflamed colon to draining lymph nodes. *Mucosal Immunol.* 11, 437–448. <https://doi.org/10.1038/mi.2017.64>.
60. King, K.Y., and Goodell, M.A. (2011). Inflammatory modulation of HSCs: viewing the HSC as a foundation for the immune response. *Nat. Rev. Immunol.* 11, 685–692. <https://doi.org/10.1038/nri3062>.
61. Castro-Dopico, T., Fleming, A., Dennison, T.W., Ferdinand, J.R., Harcourt, K., Stewart, B.J., Cader, Z., Tuong, Z.K., Jing, C., Lok, L.S.C., et al. (2020). GM-CSF Calibrates Macrophage Defense and Wound Healing Programs during Intestinal Infection and Inflammation. *Cell Rep.* 32, 107857. <https://doi.org/10.1016/j.celrep.2020.107857>.
62. Pearson, C., Thornton, E.E., McKenzie, B., Schaupp, A.L., Huskens, N., Griseri, T., West, N., Tung, S., Seddon, B.P., Uhlig, H.H., et al. (2016). ILC3 GM-CSF production and mobilisation orchestrate acute intestinal inflammation. *eLife* 5, e10066. <https://doi.org/10.7554/eLife.10066>.
63. Kasahara, S., Jhingran, A., Dhingra, S., Salem, A., Cramer, R.A., and Hohl, T.M. (2016). Role of Granulocyte-Macrophage Colony-Stimulating Factor Signaling in Regulating Neutrophil Antifungal Activity and the Oxidative Burst During Respiratory Fungal Challenge. *J. Infect. Dis.* 213, 1289–1298. <https://doi.org/10.1093/infdis/jiw054>.
64. Jia, L.G., Bamias, G., Arseneau, K.O., Burkly, L.C., Wang, E.C.Y., Gruszka, D., Pizarro, T.T., and Cominelli, F. (2016). A Novel Role for TL1A/DR3 in Protection against Intestinal Injury and Infection. *J. Immunol.* 197, 377–386. <https://doi.org/10.4049/jimmunol.1502466>.
65. Buttó, L.F., Jia, L.G., Arseneau, K.O., Tamagawa, H., Rodriguez-Palacios, A., Li, Z., De Salvo, C., Pizarro, T.T., Bamias, G., and Cominelli, F. (2019). Death-Domain-Receptor 3 Deletion Normalizes Inflammatory Gene Expression and Prevents Ileitis in Experimental Crohn's Disease. *Inflamm. Bowel Dis.* 25, 14–26. <https://doi.org/10.1093/ibd/izy305>.
66. Kirchberger, S., Royston, D.J., Boulard, O., Thornton, E., Franchini, F., Szabady, R.L., Harrison, O., and Powrie, F. (2013). Innate lymphoid cells sustain colon cancer through production of interleukin-22 in a mouse model. *J. Exp. Med.* 210, 917–931. <https://doi.org/10.1084/jem.20122308>.
67. Goc, J., Lv, M., Bessman, N.J., Flamar, A.L., Sahota, S., Suzuki, H., Teng, F., Putzel, G.G.; JRI; Live; Cell Bank, and Eberl, G., et al. (2021). Dysregulation of ILC3s unleashes progression and immunotherapy resistance in colon cancer. *Cell* 184, 5015–5030.e16. <https://doi.org/10.1016/j.cell.2021.07.029>.
68. Su, H., Cai, T., Zhang, S., Yan, X., Zhou, L., He, Z., Xue, P., Li, J., Zheng, M., Yang, X., et al. (2021). Identification of hub genes associated with neutrophils infiltration in colorectal cancer. *J. Cell. Mol. Med.* 25, 3371–3380. <https://doi.org/10.1111/jcmm.16414>.
69. Xie, X., Shi, Q., Wu, P., Zhang, X., Kambara, H., Su, J., Yu, H., Park, S.Y., Guo, R., Ren, Q., et al. (2020). Single-cell transcriptome profiling reveals neutrophil heterogeneity in homeostasis and infection. *Nat. Immunol.* 21, 1119–1133. <https://doi.org/10.1038/s41590-020-0736-z>.
70. Mortha, A., Remark, R., Del Valle, D.M., Chuang, L.S., Chai, Z., Alves, I., Azevedo, C., Gaifern, J., Martin, J., Petralia, F., et al. (2022). Neutralizing Anti-Granulocyte Macrophage-Colony Stimulating Factor Autoantibodies Recognize Post-Translational Glycosylations on Granulocyte Macrophage-Colony Stimulating Factor Years Before Diagnosis and Predict Complicated Crohn's Disease. *Gastroenterology* 163, 659–670. <https://doi.org/10.1053/j.gastro.2022.05.029>.
71. Balmer, M.L., Schürch, C.M., Saito, Y., Geuking, M.B., Li, H., Cuenca, M., Kovtonyuk, L.V., McCoy, K.D., Hapfelmeier, S., Ochsenbein, A.F., et al. (2014). Microbiota-derived compounds drive steady-state granulopoiesis via MyD88/TICAM signaling. *J. Immunol.* 193, 5273–5283. <https://doi.org/10.4049/jimmunol.1400762>.
72. Khosravi, A., Yáñez, A., Price, J.G., Chow, A., Merad, M., Goodridge, H.S., and Mazmanian, S.K. (2014). Gut microbiota promote hematopoiesis to

- control bacterial infection. *Cell Host Microbe* 15, 374–381. <https://doi.org/10.1016/j.chom.2014.02.006>.
73. Robles-Vera, I., Jarit-Cabanillas, A., Brandi, P., Martínez-López, M., Martínez-Cano, S., Rodrigo-Tapias, M., Femenía-Muiña, M., Redondo-Urzaíñqui, A., Nuñez, V., González-Correa, C., et al. (2025). Microbiota translocation following intestinal barrier disruption promotes Mincle-mediated training of myeloid progenitors in the bone marrow. *Immunity* 58, 381–396.e9. <https://doi.org/10.1016/j.jimmuni.2024.12.012>.
74. Dieckgraefe, B.K., and Korzenik, J.R. (2002). Treatment of active Crohn's disease with recombinant human granulocyte-macrophage colony-stimulating factor. *Lancet* 360, 1478–1480. [https://doi.org/10.1016/S0140-6736\(02\)11437-1](https://doi.org/10.1016/S0140-6736(02)11437-1).
75. Korzenik, J.R., Dieckgraefe, B.K., Valentine, J.F., Hausman, D.F., and Gilbert, M.J.; Sargramostim in Crohn's Disease Study Group (2005). Sargramostim for active Crohn's disease. *N. Engl. J. Med.* 352, 2193–2201. <https://doi.org/10.1056/NEJMoa041109>.
76. Jacob, N., Kumagai, K., Abraham, J.P., Shimodaira, Y., Ye, Y., Luu, J., Blackwood, A.Y., Castanon, S.L., Stamps, D.T., Thomas, L.S., et al. (2020). Direct signaling of TL1A-DR3 on fibroblasts induces intestinal fibrosis in vivo. *Sci. Rep.* 10, 18189. <https://doi.org/10.1038/s41598-020-75168-5>.
77. Louis, C., Souza-Fonseca-Guimaraes, F., Yang, Y., D'Silva, D., Kratina, T., Dagley, L., Hediyyeh-Zadeh, S., Rautela, J., Masters, S.L., Davis, M.J., et al. (2020). Correction: NK cell-derived GM-CSF potentiates inflammatory arthritis and is negatively regulated by CIS. *J. Exp. Med.* 217, e2019142103192020c. <https://doi.org/10.1084/jem.2019142103192020c>.
78. Lin, C.C., Bradstreet, T.R., Schwarzkopf, E.A., Sim, J., Carrero, J.A., Chou, C., Cook, L.E., Egawa, T., Taneja, R., Murphy, T.L., et al. (2014). Blh1e40 controls cytokine production by T cells and is essential for pathogenicity in autoimmune neuroinflammation. *Nat. Commun.* 5, 3551. <https://doi.org/10.1038/ncomms4551>.
79. Stephens, A.S., Stephens, S.R., and Morrison, N.A. (2011). Internal control genes for quantitative RT-PCR expression analysis in mouse osteoblasts, osteoclasts and macrophages. *BMC Res. Notes* 4, 410. <https://doi.org/10.1186/1756-0500-4-410>.
80. Chassaing, B., Aitken, J.D., Malleshappa, M., and Vijay-Kumar, M. (2014). Dextran sulfate sodium (DSS)-induced colitis in mice. *Curr. Protoc. Immunol.* 104, 15.25.1–15.25.14. <https://doi.org/10.1002/0471142735.im1525s104>.
81. Pires, S., and Parker, D. (2018). IL-1beta activation in response to *Staphylococcus aureus* lung infection requires inflammasome-dependent and independent mechanisms. *Eur. J. Immunol.* 48, 1707–1716. <https://doi.org/10.1002/eji.201847556>.
82. Diehl, G.E., Longman, R.S., Zhang, J.X., Breart, B., Galan, C., Cuesta, A., Schwab, S.R., and Littman, D.R. (2013). Microbiota restricts trafficking of bacteria to mesenteric lymph nodes by CX(3)CR1(hi) cells. *Nature* 494, 116–120. <https://doi.org/10.1038/nature11809>.
83. Espinosa, V., Dutta, O., McElrath, C., Du, P., Chang, Y.J., Cicciarelli, B., Pitler, A., Whitehead, I., Obar, J.J., Durbin, J.E., et al. (2017). Type III interferon is a critical regulator of innate antifungal immunity. *Sci. Immunol.* 2, eaan5357. <https://doi.org/10.1126/sciimmunol.aan5357>.
84. Dobin, A., Davis, C.A., Schlesinger, F., Drenkow, J., Zaleski, C., Jha, S., Batut, P., Chaisson, M., and Gingeras, T.R. (2013). STAR: ultrafast universal RNA-seq aligner. *Bioinformatics* 29, 15–21. <https://doi.org/10.1093/bioinformatics/bts635>.
85. Trapnell, C., Williams, B.A., Pertea, G., Mortazavi, A., Kwan, G., van Baren, M.J., Salzberg, S.L., Wold, B.J., and Pachter, L. (2010). Transcript assembly and quantification by RNA-Seq reveals unannotated transcripts and isoform switching during cell differentiation. *Nat. Biotechnol.* 28, 511–515. <https://doi.org/10.1038/nbt.1621>.
86. Trapnell, C., Hendrickson, D.G., Sauvageau, M., Goff, L., Rinn, J.L., and Pachter, L. (2013). Differential analysis of gene regulation at transcript resolution with RNA-seq. *Nat. Biotechnol.* 31, 46–53. <https://doi.org/10.1038/nbt.2450>.
87. Anders, S., Pyl, P.T., and Huber, W. (2015). HTSeq—a Python framework to work with high-throughput sequencing data. *Bioinformatics* 31, 166–169. <https://doi.org/10.1093/bioinformatics/btu638>.
88. Hassan-Zahraee, M., Ye, Z., Xi, L., Baniecki, M.L., Li, X., Hyde, C.L., Zhang, J., Raha, N., Karlsson, F., Quan, J., et al. (2022). Antitumor Necrosis Factor-like Ligand 1A Therapy Targets Tissue Inflammation and Fibrosis Pathways and Reduces Gut Pathobionts in Ulcerative Colitis. *Inflamm. Bowel Dis.* 28, 434–446. <https://doi.org/10.1093/ibd/izab193>.
89. Murray, G.I., Burke, M.D., and Ewen, S.W. (1987). Glutathione localisation in benign and malignant human breast lesions. *Br. J. Cancer* 55, 605–609. <https://doi.org/10.1038/bjc.1987.123>.
90. He, S., Bhatt, R., Brown, C., Brown, E.A., Buhr, D.L., Chantranuvatana, K., Danaher, P., Dunaway, D., Garrison, R.G., Geiss, G., et al. (2022). Highplex imaging of RNA and proteins at subcellular resolution in fixed tissue by spatial molecular imaging. *Nat. Biotechnol.* 40, 1794–1806. <https://doi.org/10.1038/s41587-022-01483-z>.
91. Hao, Y., Stuart, T., Kowalski, M.H., Choudhary, S., Hoffman, P., Hartman, A., Srivastava, A., Molla, G., Madad, S., Fernandez-Granda, C., et al. (2024). Dictionary learning for integrative, multimodal and scalable single-cell analysis. *Nat. Biotechnol.* 42, 293–304. <https://doi.org/10.1038/s41587-023-01767-y>.
92. Erben, U., Loddenkemper, C., Doerfel, K., Spieckermann, S., Haller, D., Heimesaat, M.M., Zeitz, M., Siegmund, B., and Kühl, A.A. (2014). A guide to histomorphological evaluation of intestinal inflammation in mouse models. *Int. J. Clin. Exp. Pathol.* 7, 4557–4576.

STAR★METHODS

KEY RESOURCES TABLE

REAGENT or RESOURCE	SOURCE	IDENTIFIER
Antibodies		
Live/Dead cell stain kit	ThermoFisher Scientific	Cat# L34962
CD45-AF700 (clone 30-F11)	BioLegend	Cat# 103127; RRID: AB_493714
CD45.1-FITC (clone A20)	BioLegend	Cat# 110706; RRID: AB_313495
CD45.2-PE (clone 104)	ThermoFisher Scientific	Cat# 12-0454-81; RRID: AB_465678
ROR γ t-PE (clone B2D)	ThermoFisher Scientific	Cat# 12-6981-82; RRID: AB_10807092
ROR γ t-APC (clone B2D)	ThermoFisher Scientific	Cat# 17-6981-82; RRID: AB_2573254
DR3-PE (clone 4C12)	BioLegend	Cat# 144405; RRID: AB_2561688
CD3-AlexaFluor700 (clone 17A2)	ThermoFisher Scientific	Cat# 56-0032-82; RRID: AB_529507
CD4-APC-eFluor780 (clone RM4-5)	ThermoFisher Scientific	Cat# 47-0042-82; RRID: AB_1272183
CD127 (IL-7Ra)-Pe-Cy7 (clone A7R34)	ThermoFisher Scientific	Cat# 25-1271-82; RRID: AB_469649
CD90.2 (Thy1.2)-APC (clone 53-2.1)	ThermoFisher Scientific	Cat# 17-0902-81; RRID: AB_469421
KLRG1-APC-eFluor780 (clone 2F1)	ThermoFisher Scientific	Cat# 47-5893-82; RRID: AB_2573988
GM-CSF-BV421 (clone MP1-22E9)	BD Biosciences	Cat# 564747; RRID: AB_2738929
Ly6G-PerCP-Cy5.5 (clone 1A8)	BioLegend	Cat# 127616; RRID: AB_1877271
CD11b-APC-eFluor780 (clone M1/70)	ThermoFisher Scientific	Cat# 47-0112-82; RRID: AB_1603193
Siglec-F (CD170)-Pe-Cy7 (clone S17007L)	BioLegend	Cat# 155527; RRID: AB_2890715
Ly6C-BV421 (clone HK1.4)	ThermoFisher Scientific	Cat# 48-5932-82; RRID: AB_10805519
Ly6C-BV650 (clone HK1.4)	BioLegend	Cat# 128036; RRID: AB_2562353
CD14-PE (clone 155527)	ThermoFisher Scientific	Cat# 12-0141-81; RRID: AB_465562
CD177-AF647 (clone Y127)	BD Biosciences	Cat# 566599; RRID: AB_2869790
PD-L1-BV421 (clone10F.9G2)	BioLegend	Cat# 124315; RRID: AB_10897097
anti-mouse Lineage Cocktail-AF700	BioLegend	Cat# 133313; RRID: AB_2715571
Sca-1 (Ly6A/E)-Pe-Cy7 (clone D7)	ThermoFisher Scientific	Cat# 25-5981-82; RRID: AB_469669
C-Kit (CD177)-APC (clone 2B8)	BioLegend	Cat# 105811; RRID: AB_313220
CD16/32-FITC (clone 2.4G2)	BD Biosciences	Cat# 561728; RRID: AB_10894390
CD34-PerCP-Cy5.5 (clone MEC14.7)	BioLegend	Cat# 119327; RRID: AB_2728136
CD150 (SLAM)-PE (clone TC15-12F12.2)	BioLegend	Cat# 115904; RRID: AB_313683
Flt3 (CD135)-BV421 (clone A2F10.1)	BD Biosciences	Cat# 562898; RRID: AB_2737876
CD48-PerCP-Cy5.5 (clone HM48-1)	BioLegend	Cat# 103421; RRID: AB_1575045
CD-38-PeCy7 anti-human (clone HIT2)	BioLegend	Cat# 303516; RRID: AB_2072782
CD90 (Thy1)-PE anti-human (Clone 5E10)	BioLegend	Cat# 328110; RRID: AB_893433
CD49f-Pacific Blue anti-human (clone GoH3)	BioLegend	Cat# 313620; RRID: AB_2128018
CD34-FITC anti-human (clone AC136)	Miltenyi biotec	Cat# 130-113-178; RRID: AB_2726005
CD45RA-APC-Cy7 anti-human (clone HI100)	BioLegend	Cat# 304128; RRID: AB_10708880
Precision counting beads™	BioLegend	Cat# 424902
Biological samples		
Human PBMCs	Weill Cornell Medicine	IRB# 1501015812
Paraffin-embedded tissue blocks	Amsterdam University Medical Center and OLVG hospital	Medical ethical committee 363 Amsterdam UMC
Chemicals, recombinant proteins, and blocking antibodies		
Phorbol myristate acetate	Sigma-Aldrich	Cat# P1585
Ionomycin calcium salt	Sigma-Aldrich	Cat# I0634
GolgiPlug	BD Bioscience	Cat# 51-2301KZ
SYBR Green Supermix	Roche	Cat# 4887352001

(Continued on next page)

Continued

REAGENT or RESOURCE	SOURCE	IDENTIFIER
0.5M EDTA pH8.0	Invitrogen	Cat# AM9261
DL-Dithiothreitol	Sigma-Aldrich	Cat# D9779
RPMI without L-glutamine	GE Healthcare	Cat# SH30096.01
Sodium pyruvate	Sigma-Aldrich	Cat# S8636
L-glutamine	Corning Life Sciences	Cat# 25-005-Cl
Penicillin/Streptomycin	HyClone	Cat# SV30010
2-mercaptoethanol	Gibco	Cat# 21985-023
HEPES	HyClone	Cat# SH30237.01
Collagenase 8	Sigma-Aldrich	Cat# C2139
Deoxyribonuclease I from bovine pancreas	Sigma-Aldrich	Cat# DN25
Percoll	GE Health	Cat# 17-0891-01
Formalin	Sigma-Aldrich	Cat# 65346
Histopaque 1119	Sigma-Aldrich	Cat# 11191
Histopaque 1077	Sigma-Aldrich	Cat# 10771
Azoxymethane	Sigma-Aldrich	Cat# A5486
Dextran sulfate sodium salt	ThermoFisher Scientific	Cat# J14489.22
Ultra LEAF purified anti-mouse DR3 (TNFRSF25)	Biolegend	Cat# 144411
InVivoMAb anti-mouse Ly6G	BioXCell	Cat# BE0075-1
InVivoMAb anti-mouse GM-CSF	BioXCell	Cat# BE0259
InVivoMAb anti-mouse/rat IL-17A	BioXCell	Cat# BE0173
Mouse IL-22 Antibody	R&D	Cat# MAB5821
Recombinant Mouse TL1A/TNFSF15	R&D	Cat# 1896-TL-010/CF
Recombinant Murine IL-6	PeproTech	216-16
Recombinant Human TGF- β 1	PeproTech	100-21

Critical commercial assays

All prep DNA/RNAMini Kit	QIAGEN	Cat# 80204
RNeasy Plus Micro Kit	QIAGEN	Cat# 74034
iScript cDNA synthesis kit	Bio-Rad	Cat# 1708891
Taqman SNP Genotyping Assays	ThermoFisher Scientific	Cat# C_1305297_10Cat#C_11277159_10
FoxP3/Transcription Factor Staining Buffer set	eBioscience	Cat# 00-5523-00
Fixation/Permeabilization Concentrate	ThermoFisher Scientific	Cat# 00-5123-43
Fixation/Permeabilization Diluent	ThermoFisher Scientific	Cat# 00-5223-56
CM-H2DCFDA (General Oxidative Stress Indicator)	ThermoFisher Scientific	Cat# C6827
Anti-Cy7 MicroBeads	Miltenyi Biotec	Cat# 130-091-652
LD columns	Miltenyi Biotec	Cat# 130-042-901

Deposited data

Neutrophils RNA-seq	NCBI	GSE248113
Spatial Transcriptomics	Zenodo	https://doi.org/10.5281/zenodo.15933207
Digital Spatial Profiling	Zenodo	https://doi.org/10.5281/zenodo.16102305

Experimental models: Cell lines

Cell line: MC38	Dr. Greg Sonnenberg, WCM	N/A
-----------------	--------------------------	-----

Experimental models: Organisms/strains

Mouse: C57BL/6	Jackson Laboratories	Cat# 000664
Mouse: Rorc-Cre	Jackson Laboratories	Cat# 022791
Mouse: Rag2 ^{-/-}	Jackson Laboratories	Cat# 008449
Mouse: Itgax-Cre	Jackson Laboratories	Cat# 008068
Mouse: Cd4-Cre	Jackson Laboratories	Cat# 022071
Mouse: KikGR33	Jackson Laboratories	Cat# 013753
Mouse: Rag2 ^{-/-} /Il2rg ^{-/-}	Taconic Farms	Cat# 4111

(Continued on next page)

Continued

REAGENT or RESOURCE	SOURCE	IDENTIFIER
Mouse: <i>Tnfrsf15</i> ^{flox/flox} <i>Tnfrsf25</i> ^{flox/flox} ; <i>Tnfrsf25</i> ^{-/-}	Castellanos et al. ¹¹ and Jacob et al. ⁷⁶	N/A
Mouse: <i>Csf2</i> ^{flox/flox}	Louis et al. ⁷⁷	N/A
Oligonucleotides		
<i>Cebpa</i> : 5'- CAAAGCCAAGAACGGTGGGA -3'; 5'- CCTTCTGTTGCGTCTCCACGTT-3'	Origene	N/A
<i>Cebpb</i> : 5'- AGCCCCTACCTGGAGGCCGCTCGCG -3'; 5'- GCGCAGGGCGAACGGGAAACCG -3'	Origene	N/A
<i>Tnfrsf25</i> : 5'- TCGGACACCTTCTTGACCAGAG -3' 5'- TCCGACTTTGCCGAGCAGTTCT -3'	Origene	N/A
<i>Csf2</i> : 5'- GCCATCAAAGAACGCCCTGAA -3' 5'- GCGGGTCTGCACACATGTTA -3'	Lin et al. ⁷⁸	N/A
<i>Hprt</i> : 5'-GAGGAGTCCTGTTGATGTTGCCAG-3' 5'-GGCTGGCCTATAAGGCTCATAGTGC-3'	Stephens et al. ⁷⁹	N/A
Software and algorithms		
R 4.4.0	RStudio	N/A
Seurat 5.1.0	Seurat	N/A
dbscan 1.2.2	dbscan	N/A
GraphPad Prism 10	GraphPad Software	N/A
FlowJo LLC v10.10	Becton Dickenson	N/A

EXPERIMENTAL MODEL AND STUDY PARTICIPANT DETAILS

Human PBMCs

Peripheral blood mononuclear cells (PBMCs) of individuals with Crohn's disease were obtained from the JRI IBD Live Cell Bank Consortium at Weill Cornell Medicine following protocols approved by the Institutional Review Board (IRB No. 1501015812). Informed consent was obtained from all subjects. Isolation of human PBMCs and single-cell suspensions was achieved by Ficoll-Paque (GE Healthcare) density gradient centrifugation.

Digital spatial RNA profiling

Paraffin-embedded tissue blocks were retrieved from the pathology archives of Amsterdam University Medical Center and OLVG hospital (Amsterdam, the Netherlands). Samples were obtained from endoscopic- or resections from patients with inflammatory bowel disease (IBD) (n=9) and non-IBD (n=3) with dysplasia. Subject characteristics are provided in Table S3. This study was approved by the medical ethical committee METC 363 Amsterdam UMC, and all patients provided informed consent.

Colitis and colorectal tumor models

DSS-induced colitis

To induce chemical colitis in mice, 2% DSS (w/v) (M.W. 40,000) was added to sterile drinking water for 6 days. After 6 days, DSS was replaced with normal drinking water.

AOM/DSS colitis-induced tumor model

The AOM/DSS model was established using a protocol previously described.³⁰ Briefly, mice were given an initial intraperitoneal injection of 10 mg/kg AOM, followed by 2% DSS treatment on day 5 after AOM injection. DSS treatment was repeated twice (five days of 2.5% DSS and four days of 2% DSS), with 14 days interval between cycles.

Heterotopic MC38 colorectal cancer cell line

2.5x10⁵ or 5x10⁵ MC38 cells were injected alone or mixed with either 50k sorted colonic neutrophils or 50k sorted bone marrow neutrophils subcutaneously into either *Rag*-deficient or WT mice.

METHOD DETAILS

Mice

C57BL/6J (Jax 000664), *Itgax*-Cre (CD11c) (JAX 008068), *Rorc*-Cre (JAX 022791), and *Rag2*^{-/-} (JAX 008449) mice were purchased from The Jackson Laboratory. *Tnfrsf25*^{-/-}, *Tnfrsf25*^{flox/flox} and *Tnfrsf15*^{flox/flox} mice were provided by S. Targan.^{11,76} *Csf2*^{flox/flox} mice were provided by Ian Wicks.⁷⁷ *Csf2*^{flox/flox} *Rorc*-Cre mice were also backcrossed to *Rag2*-deficient animals to generate *Csf2*^{flox/flox} *Rorc*-Cre *Rag2*^{-/-} mice. CD4-cre mice were obtained from Jackson Laboratory and crossed with *Tnfrsf25*^{flox/flox} mice. *Rag2*^{-/-}*Il2rg*^{-/-} (4111) mice were purchased from Taconic Farms. KikGR 33 mice were purchased from Jackson laboratory

(JAX 013753). Mice were maintained under SPF conditions. Littermate controls were used for each experiment. All mice used were between 6 and 10 weeks old, and age- and sex-matched for each experiment. For AOM/DSS experiments, female mice were used to preserve overall survival, given increased male mice susceptibility to DSS.⁸⁰ All mice were bred in-house under standard conditions at the animal facility of Weill Cornell Medicine (WCM). All protocols were approved by the Institutional Animal Care and Use Committee at WCM and MSKCC, and all experiments were performed in accordance with the established guidelines.

Bone Marrow isolation of neutrophils

Neutrophils were isolated from the bone marrow of the femurs and tibias of naive WT mice by density gradient centrifugation as previously described.⁸¹ Briefly, bone marrow cells were flushed from the bone with RPMI media supplemented with 10%FBS and 2mM EDTA. Red blood cell lysis was performed using a sodium chloride solution (0.2% followed by 1.6% for 40sec) to avoid neutrophil activation. Bone marrow cells were then washed and overlaid on a Histopaque 1119 and Histopaque 1077 gradient (Sigma) and centrifuged for 30 min at 720 x g at room temperature without brake. Neutrophils were collected at the interface between the two layers and after assessment of cell number and viability, neutrophils were resuspended in HBSS without calcium and magnesium. Neutrophil purity was confirmed by flow cytometry.

Murine intestinal immune cell isolation

Lamina propria cells were isolated from small intestine and colon tissue as previously described.⁸² Briefly, colon was removed, opened longitudinally, rinsed with ice-cold PBS and cut into approximately 1.5 cm pieces. To remove intestinal epithelial cells tissue was incubated in PBS (Sigma-Aldrich) containing 1 mM DTT (Sigma-Aldrich) at 200 rpm for 10 min at room temperature, followed by 10 min incubation at 200 rpm at 37°C with 30 mM EDTA (Thermo Fisher Scientific), and 10mM HEPES (Invitrogen) which was performed twice. Samples were rinsed in RPMI media and the remaining tissues were enzymatically digested in R10 media containing 100 U/ml type VIII collagenase (Sigma-Aldrich) and 150ug/ml DNase I (Sigma-Aldrich) in a shaker for 45 min at 37°C.

Intestinal ILC isolation

Lineage⁻ KLRG1⁺ NK1.1⁺ CD90^{hi} CD127⁺ mouse ILC3s were sorted from LPMCs¹¹ and resuspended in R10 (RPMI1640 supplemented with 10% FBS, 2mM L-Glutamine, Penicillin/Streptomycin, 10mM HEPES buffer, 1mM sodium pyruvate, 0.5X MEM amino acids and 2-mercaptoethanol) tissue culture media for stimulation directly *ex vivo*.

Cell depletion

For neutrophil depletion during AOM/DSS, mice were injected intraperitoneally either with 250 µg of anti-mouse Ly6G (clone 1A8; Bio X Cell) or with IgG2a, κ isotype control (clone 2A3; Bio X Cell) every 5 days for 6 times starting with the first day of the first round of DSS.

Flow cytometry staining and analyses

For flow cytometry analysis, unlabelled anti-CD16/32 (clone 2.4G2, BD Biosciences) was used to block Fc receptors and dead cells were excluded using Live/Dead Fixable Aqua Dead Cell Stain (Thermo Fisher Scientific). The staining antibodies for flow cytometry were purchased from Biolegend or BD Biosciences. The following were used for mouse cell-surface staining: CD45 (30/F11), CD45.2 (104), CD11b (M1/70), LY6G (1A8), SIGLECF (S17007L), CD90.2 (53-2.1), CD127 (A7R34), NK1.1 (PK136), KLRG1 (2F1), LIN- (CD3/LY6G/LY6C/CD11B/B220/Ter-119), SCA-1 (D7), C-KIT (2B8), CD16/32 (2.4G2), CD48 (HM48-1), CD150 (TC15-12F12.2), CD135 (Flt3- A2F10.1), CD14 (Sa2-8). The following were used for mouse intracellular staining: RORyt (B2D), GM-CSF (MP1-22E9). The following were used for cell-surface staining of human samples: LIN- (CD3, CD14, CD16, CD19, CD20, CD56), CD49F (GoH3), CD90 (5E10), CD34 (AC136), CD38 (HIT2), CD45RA (HI100). Human GMPs cells were gated as GMPs (Lin⁻ CD34⁺ CD38⁺ CD45RA⁺).

For transcription factor detection, cells were stained for surface markers before fixation and permeabilization with Intracellular Fixation and Permeabilization kit as per manufacturer's instructions (eBiosciences) for intracellular staining. For cytokine detection, cells were stimulated with phorbol myristate acetate (PMA, 20ng/mL) and ionomycin (1µg/mL) in the presence of BD GolgiPlug for 3 hours at 37°C before staining. Following surface-marker staining cells were prepared as per manufacturer's instruction with Cytofix/Cytoperm buffer set (BD Biosciences) for intracellular cytokine evaluation. For ROS detection cells were treated as previously described.⁸³ Briefly, cells were cultured with 1.0 µM CM-H2DCFDA (Life Technologies) in Hanks' balanced salt solution for 45 min at 37°C. After incubation, cells were stained with neutrophil markers and analyzed using flow cytometry. Cell number was quantified using counting beads (Precision counting beads™, Biolegend) according to the manufacturer's instructions. Data acquisition was computed with BD LSRII flow cytometer and analysis performed with FlowJo software (Tree Star).

Co-culture assays

Sort-purified intestinal ILC3 (2×10^3 or 1×10^4) and bone marrow derived neutrophils (2×10^4 or 1×10^5) were co-cultured together at a ratio of 1:10 in a 96-well round-bottom tissue culture plate with R10 media supplemented with IL-6 (20ng/mL) and TGF-β (2ng/mL) in the presence or absence of 100 ng/mL rTL1A. Cultures were incubated at 37°C for 18h. For co-cultures using supernatants, sort purified ILC3s were stimulated overnight for 18h at 37°C after which supernatants were collected and used to stimulate freshly purified neutrophils for 18h at 37°C. For either GM-CSF, IL-22 or IL-17 blockade, 200 ng of blockade antibodies were added to the overnight

co-culture. To test the tumor promoting capacity in vivo, 100k neutrophils were stimulated overnight as described and injected i.v. every 7 days for 4 weeks during AOM/DSS starting on second day of the first round of DSS.

Cytokine quantification

Cytokine concentrations in the serum (50–100 µL), bone marrow extracellular fluid (100 µL) and ILC3 supernatants (100 µL) were quantified by multiplex analysis (Mouse 32-plex; Eve Technologies).

Bone marrow progenitor isolation and ex vivo stimulation

LSKs and GMPs were FACS-sorted. Briefly, pre-enrichment of progenitors was obtained by depletion of Lin⁺ cells using Miltenyi Biotech microbeads and LD columns. LSKs were sorted as live Lin⁻ Sca-1⁺ C-kit⁺ and GMPs as live Lin⁻ Sca-1⁻ C-kit⁺ CD150⁻ CD16/32⁺ CD34⁺. 20k LSKs and 25k GMPs were sorted and used either directly for RNA extraction to assess transcription of *Cebpa*, *Cebpb*, and *Tnfrsf25* or stimulated overnight in 200µL of R10 media supplemented with 50 µL of serum collected at day 1 from mice treated either with α-IgG or α-DR3.

Tracking of intestinal cell trafficking by photoconversion of KikGR33 mice

To track cell migration from the gut, intestinal tissue of KikGR33 mice was exposed to a 405nm UV laser as previously described.⁵⁸ Briefly, KikGR33 mice were anesthetized with 2.5% isoflurane (vol/vol) delivered in 2l/min of O₂ and maintained at 37C throughout the procedure. A 2 cm incision was made in the abdominal wall and the cecum was placed onto a sterile aluminum foil square. Both sides of the cecum were exposed to the laser (405nm, at 400mW output) for 2.5 minutes each. Sterile saline was continuously applied to maintain hydration. The cecum was returned to the abdominal cavity and the incision sutured. 2 days after surgery, the bone marrow was analyzed by flow cytometry for presence of photoconverted RFP⁺ cells that migrated from the cecum.

RNA-seq

RNA from bone marrow purified neutrophils and sorted intestinal ILC3s was extracted and purified using RNeasy Plus Mini Kit (Qiagen). For RNA-sequencing of bone marrow derived neutrophils, 1x10⁵ cells were stimulated for 18h with ILC3s supernatants. ILC3 supernatants were obtained from 2×10³ of sort-purified intestinal ILC3s unstimulated or stimulated for 18h with TL1A. For neutrophils, libraries were generated using SMART-Seq® v4 Ultra® Low Input RNA Kit and sequenced with paired-end 50 bps on NovaSeq6000 sequencer at the Genomics core (Weill Cornell Medicine). The raw sequencing reads in BCL format were processed through bcl2fastq 2.20 (Illumina) for FASTQ conversion and demultiplexing. After trimming the adaptors with cutadapt (version1.18) (<https://cutadapt.readthedocs.io/en/v1.18/>), RNA reads were aligned and mapped to the GRCm38 mouse reference genome by STAR (Version2.5.2) (<https://github.com/alexdobin/STAR>),⁸⁴ and transcriptome reconstruction was performed by Cufflinks (Version 2.1.1) (<http://cole-trapnell-lab.github.io/cufflinks/>). The abundance of transcripts was measured with Cufflinks in Fragments Per Kilobase of exon model per Million mapped reads (FPKM).^{85,86} Raw read counts per gene were extracted using HTSeq-count v0.11.2.⁸⁷ Gene expression profiles were constructed for differential expression, cluster, and principal component analyses with the DESeq2 package (<https://bioconductor.org/packages/release/bioc/html/DESeq2.html>). RNA-seq data generated from colonic biopsies from a Phase 2a study evaluating the role for anti-TL1A therapy in the treatment of moderate to severe UC was described previously.⁸⁸

CosMx spatial molecular imaging analysis pipeline

3 mm tissue cores from FFPE blocks of colonic tissue were used to construct a tissue microarray at the Center for Translational Pathology within a 15 x 20 mm space. Slides were dried overnight at 37°C and moved into a desiccator the following day. Sections of the TMA were desiccated and analyzed immediately by CosMx spatial molecular imaging. Tissue microarray sectioning, processing, staining, imaging, and downstream analysis were performed as previously described.⁸⁹ After ISH hybridization and RNA readout were completed, measurements were taken for additional markers CD45, CD298/B2M, pan-cytokeratin, and DAPI. An image stack was generated at each FOV location, and cell segmentation was performed. Within each cell's boundaries, transcript detection was performed as previously described to map each transcript to a corresponding cell.⁹⁰ Raw ISH counts were analyzed in R (v4.4) using Seurat (v5.1.0) and related packages.⁹¹ Raw counts were normalized using SCTtransform with a clipping range of -10 to 10 to stabilize variance and regress out technical effects. Dimensionality reduction was performed via principal component analysis (PCA), retaining 50 PCs for downstream analyses. Uniform Manifold Approximation and Projection (UMAP) was computed on these PCs to visualize the transcriptional landscape in two dimensions. Louvain clustering and annotation was performed in a semi-supervised manner to assess cluster stability and biological interpretability. Cluster-specific marker genes were identified and tabulated with the function FindAllMarkers. Cluster identities were manually annotated using known marker genes. Marker expression was visualized with FeaturePlot, DotPlot, ImageFeaturePlot, ImageDimPlot, and VlnPlot functions to confirm regional and cell-type specificity.

Neighborhood enrichment analysis

Analysis was used to test the spatial adjacency between a “target” cell type (neutrophils) and one or more “neighbor” cell types (e.g. neoplastic epithelium) in the spatial transcriptomics dataset. Cores with less than ten neutrophils were excluded from this analysis. Briefly, centroid coordinates for each cell were used to construct a fixed radius nearest neighbor graph using the frNN

function in the package dbSCAN (ANN: Approximate Nearest Neighbors Version: 1.1.2), which identifies for each cell i , any other cell j whose Euclidean distance $\leq 50 \mu\text{m}$. For each neighbor of cell type k , the number of edges were tallied from all neutrophil nodes to nodes of type k . To correct for differing abundances of cell types, raw edge counts were divided by the corresponding abundance of cell type k in the respective tissue core and a null distribution was generated to perform a Monte Carlo significance test. Briefly, total neutrophil count was fixed and randomly reassign “neutrophil” labels to a random sample of the same number of cells drawn uniformly from all cells. For 1,000 replicates, the normalized edge count was computed, building an empirical null distribution, which was used to compute a z-score and an empirical one-tailed p-value. The z-scores and p-values are computed for the co-localization of each neighbor cell type of interest with the target cell type (neutrophils) in each core.

Gene expression by Quantitative RT-PCR

RNA was extracted and purified as described and quantified by Nanodrop prior to reverse transcription with iScript cDNA synthesis kit (Bio-Rad). qPCR was performed on an Applied BioSciences Quant Studio 6 Flex Real-time PCR (Applied Biosystems) using PerfeCTa SYBR Green Fast mix, Low ROX (Quanta Biosciences). The following primers were used: for *Cebpa*, *Cebpa*-F 5'-GCAAAGCCAAGAACGGTGGGA-3' and *Cebpa*-R 5'- CCTTCTGTTGCGTCTCCACGTT-3'; *Cebpb*, *Cebpb*-F 5'- AGCCCCTACC TGGAGCCGCTCGCG-3' and *Cebpb*-R 5'- GCGCAGGGCGAACGGGAAACCG-3'; *Tnfrsf25*, *Tnfrsf25*-F 5'- TCGGACACCTT CTTGACCAGAG-3' and *Tnfrsf25*-R 5'- TCCGACTTTGCCGAGCAGTTCT-3' (Origene); *Csf2* *Csf2*-F 5'-GCCATCAAAGAGCCCT GAA-3', *Csf2*-R 5'-GCGGGTCTGCACACATGTTA-3⁷⁸ and *Hprt*, *Hprt*-F 5' GAGGAGTCCTGTTGATGTTGCCAG3' and *Hprt*-R 5' GGCTGGCCTATAAGGCTATAGTGC3'.⁷⁹ The thermocycler program was as follows: initial cycle of 95C for 60 s, followed by 40 PCR cycles at 95C for 5 s, 60C for 15 s, 72C for 15 s. Relative levels of the target genes were determined by calculating the DCt to housekeeping gene *Hprt* expression.

Histological analysis and colitis scoring

Intestinal tissue was fixed in 10% formalin and embedded in paraffin. For hematoxylin and eosin (H&E) staining, standard histological techniques were used. H&E sections of the colon were analyzed for tumors by a blinded reader (C.N. or R.L.). Colitis severity was scored as previously defined for chemically-induced colonic inflammation by the extent of inflammatory cell infiltrate (mild mucosal as a 1, moderate mucosal and submucosal as a 2, and marked transmural as a 3) and epithelial architecture changes (focal erosions as a 1, erosions +/- focal erosions as a 2, extended ulcerations +/- granulation tissue +/- pseudopolyps as a 3).⁹² The sum of these individual scores per sample is reported.

TNFSF15 SNP genotyping

Genomic DNA was extracted and purified from human PBMCs using All prep® DNA/RNA Mini Kit (Qiagen). Samples were genotyped using Taqman SNP Genotyping Assays (rs6478109, C_1305297_10; rs7848647, C_11277159_10) and Taqman Genotyping Master Mix according to the manufacturer's protocol on an Applied BioSciences Quant Studio 6 Flex Real-time PCR (Applied Biosystems).

Digital spatial RNA profiling

Hematoxylin and eosin (H&E) slides from each patient block were annotated by a dedicated IBD pathologist to define areas of dysplasia. A 2 mm core was then extracted from each block and embedded in a new paraffin block to create a tissue microarray (TMA). Two TMA slides (4 μm thick) were incubated with the Human Whole Transcriptome Atlas panel (NanoString, USA) and subsequently stained with anti-pan-cytokeratin (AE1+AE3, Novus Biologicals), anti-CD45 (2B11+PD7/26, Novus Biologicals), and nuclear SYTO13 (NanoString, 121303303) antibodies according to the manufacturer's protocol (1). Following staining, the slides were loaded and scanned using the GeoMX instrument. 1 to 4 regions of interest (ROIs) were selected in each core, and immune cells (CD45^+) were segmented using NanoString GeoMX software. Quality control (QC) for segmental and biological probes was performed following a publicly available pipeline (2). All data pre-processing and normalization were conducted in R (version 4.2.0). After QC genes with abnormally low signals were excluded. The final gene expression matrix contained 11,151 genes. Gene expression data were normalized using the quartile 3 method from the NanoStringNCTools (v1.6.1) package and subsequently log₂-transformed. Key tumor-associated neutrophil gene markers (including *CD14*, *CEBPB*, *MPO*, *OSM*, *CCL2*, *ICAM1*, and *IL1B*) identified from our in vitro studies and published literature were analyzed in IBD-associated dysplasia compared to sporadic dysplasia. The mean Z-score was calculated using the classic z-score formula: $Z=(x-\mu/\sigma)$ (x =an individual data point, μ = dataset mean, and σ = dataset standard deviation).

Statistical analysis

Statistical tests were performed with GraphPad Prism (v.9.5.1). Statistical analyses were done using unpaired Student's t-tests with 95% confidence intervals, a one-way Anova for multiple comparisons when comparing one condition between groups or a two-way ANOVA for multiple comparisons when comparing more than two conditions of interest. For categorical histologic colitis scoring, Fisher's exact test was used for sample comparison. For differential expression analysis of RNA seq data, pairwise comparisons between two or more groups using parametric tests where read-counts follow a negative binomial distribution with a gene-specific dispersion parameter. Corrected p-values were calculated based on the Benjamini-Hochberg method to adjust for multiple testing.

A probability value of $P < 0.05$ was considered significant. To determine significant differences in expression of specific genes between non-IBD and IBD samples with digital spatial profiling, the Wilcoxon test was used, considering p-value less than 0.05 as significant, with the following levels of significance: p-value < 0.0001, ****, p-value < 0.001; **, p-value < 0.01; *, p-value < 0.05; *. To quantitatively assess the enrichment of the neutrophil signature in non-IBD versus IBD patients, a z-score was calculated per patient considering the expression of each gene in the signature. Significant differences were determined using the unpaired t-test. Statistical significance is indicated in each figure as following * $p < 0.05$, ** $p < 0.01$, *** $p < 0.001$, **** $p < 0.0001$.